UNIVERSIDADE DA BEIRA INTERIOR

Desenvolvimento de matrizes poliméricas para a aplicação na regeneração da pele

Patrícia Esteves Fernandes

Dissertação para obtenção do Grau de Mestre em

Biotecnologia

(2º ciclo de estudos)

Orientador: Prof. Doutor Ilídio Joaquim Sobreira Correia, Ph.D.

Co-orientador: Sónia Miguel
Co-orientador: Elisabete Costa

Covilhã, outubro de 2015

“Tudo aquilo que o homem ignora, não existe para ele. Por isso o universo de cada um, resume-se ao tamanho do seu saber.” —Albert Einstein

Acknowledgments

I would like to thank to my supervisor Professor Ilídio Correia for supporting the developing of my work.
I would like thank Sónia Miguel for all guindance along my practical work.
I would like to thank Elisabete Costa for all the help in the most important and final phase of my thesis.
I also would like to thank Lino Cipriano for all the support and patience over the last seven years.
I would like to thank my group colleagues for their support and to my closest friends that have always be on my side during these last years.
Lastly, and most importantly, I would like thank to my family, especially my parents and my sister for their support.

Abstract

Skin is the largest organ of the human body, and it is involved in the preservation of homeostasis of the body fluids, temperature and protection against infectious agents. When skin is injured, a complex process of regeneration begins. To promote skin regeneration it may be coated with proper biomaterials that contribute for the restoration of skin structure and functions, by reducing the risk of infection, avoiding dehydration, pain and reducing the formation of scar.
Herein, a new sponges (S) aimed to promote skin regeneration ware developed. The materials used of the production this sponge were: Chitosan and Gelatin.
Sponges were coated with a membrane (M), the materials used were deacetylated Chitosan, Poly (ethylene oxide) (PEO) and Poly (ε-caprolactone) (PCL), mimicking the natural anatomy and physiology of skin. The coated sponge (CS) produced is biocompatible, biodegradable, anti-inflammatory and antimicrobial porous structure that allow the difusion of nutrients and waste products. Furthermore, Ibuprofen was also loaded at sponges to improve the skin regenenation, by decreasing wound edema and decreased production of inflammatory mediators.
The structure of the biomaterials developed here (S, M and CS) were initially characterized by Fourier transform infrared spectroscopy (FTIR). Ther morphology was characterized by scanning electron microscopy (SEM). Cellular adhesion and internalization into the porous structures of the biomaterials were visualized by confocal laser scanning microscopy (CLSM). The cytotoxicity profile of the biomaterials were characterized through 3-(4,5-Dimethyl-2-thiazolyl)-2,5-diphenyl-2H-tetrazolium bromide (MTT) assays and the results obtained confirmed their biocompatibility. The antimicrobial activity of the sponges were also evaluated and the results showed that they were able to inhibit the growth, at the surface, of the most common microorganism in skin infection (*Staphylococcus aureus*). In conclusion, the produced porous sponges has suitable properties for improving the healing process of cutaneous wounds.

Keywords: Quitosan, skin regeneration, coated sponge, freeze drying and electrospinning.

Resumo

A pele é o maior órgão do corpo humano e este órgão está envolvido na preservação da homeostase dos fluidos corporais, manutenção da temperatura e protecção contra agentes infecciosos. Quando a estrutura da pele é comprometida inicia-se um complexo processo de regeneração. Para promover este processo a pele pode ser revestida com biomateriais com o objectivo de reduzir o risco de infecção, desidratação, dor e a formação de cicatriz.

No presente estudo foram desenvolvidas novas esponjas (S) para a regeneração da pele. Os materiais utilizados na sua produção foram: O Quitosano e a Gelatina.

Por outro lado as esponjas também foram revestidas com uma membrana (M), em que os materiais usados foram o Quitosano desacetilado, Óxido de polietileno (PEO) e policaprolactona (PCL), imitando a anatomia e fisiologia natural da pele. A esponja revestida (CS) é biocompatível, biodegradável, possi uma estrutura porosa com propriedades antimicrobianas, que permite a difusão de nutrientes e produtos residuais. Além disso, no interior do CS as células permacem viáveis e ocorre a proliferação. O Ibuprofeno foi também incorporado nas esponjas para acelarar a regeneração da pele, ao diminuir o edema da ferida por diminuição da produção de mediadores inflamatórios.

A estrutura dos biomateriais produzidos, foram analisadas por espectroscopia de infravermelho com transformada de Fourier (FTIR). A morfologia da superfície e do interior das esponjas foi caracterizada por microscopia eletrónica de varrimento (SEM). A adesão celular e internalização das células nas estruturas porosas foram visualizadas através de imagens de microscopia confocal. Os perfis citotoxidos dos biomateriais foram caracterizados por meio de ensaios de viabilidade celular, e os resultados obtidos confirmaram a sua biocompatibilidade. A actividade antimicrobiana dos biomateriais foi também avaliada e os resultados mostraram que as esponjas inibem o crescimento na sua superfície, do microrganismo mais comum das infecções de pele (*Staphylococcus aureus*). As estruturas porosas têm propriedades adequadas para melhorar o processo de cicatrização de feridas cutâneas.

Palavras-chave: Quitosano, regeneração da pele, espoja revestida, liofilização electrospining.

Resumo alargado

A pele é o maior órgão do corpo humano, representando cerca de 7 % da massa corporal, chegando a atingir uma extensão de $2m^2$ num adulto. Este tecido tem como principal função servir de barreira protetora do organismo, protegendo contra infeções. Por outro lado, este orgão também preserva a hemóstase dos fluidos do corpo humano e ajuda na regulação da temperatura corporal. A pele é constituída por três diferentes camadas: Epiderme (camada externa), Derme (camada intermédia) e Hipoderme (camada interna).

Diariamente a pele está sujeita a lesões, que podem ser causadas por queimaduras, cirurgias, traumas, contusões e hematomas. Estas lesões levam à disrupção do tecido quer a nível anatómico quer a nível funcional.

Após ocorrer uma lesão de pele, inicia-se um processo de cicatrização que tem por objectivo restabelecer as propriedades e funções nativas da pele. Este processo é complexo e envolve fases que incluem: Hemostase, Inflamação, Migração celular, Proliferação e Maturação. Com o intuito de restabelecer o mais rapidamente possível a estrutura e função da pele têm sido usados auto-, alo- e xeno- enxertos. Até ao presente foram desenvolvidos um grande número de substitutos de pele. No entanto, estas abordagens terapêuticas apresentam algumas limitações tais como, a rejeição por parte do paciente, risco de transmissão de doenças e, ainda uma disponibilidade limitada. Devido a este facto tem-se procurado desenvolver novos substitutos de pele que permitam acelerar o processo de cicatrização.

No presente estudo foi desenvolvido um novo substituto de pele, que consiste numa esponja revestida. A esponja foi produzida por um processo de congelação/descongelação. Posteriormente, esta foi revestida pelo método de electrospinning com uma membrana fibrosa, contendo um agente anti-inflamatório (Ibuprofeno). Os biomateriais escolhidos na produção da esponja revestida foram o Quitosano, Gelatina, PEO e PCL, que são conhecidos por possuírem as propriedades requeridas para serem aplicados na regeneração do tecido, como sejam, a biocompatibilidade, a actividade antimicrobiana, degradabilidade, e ainda uma porosidade que permite a internalização e a proliferação das células dentro da sua estrutura e ainda permitem a difusão de gases, nutrientes e produtos residuais. O Ibuprofeno foi ainda incorporado nas esponjas para reduzir a inflamação associada à lesão.

A estrutura dos biomateriais produzidos, foram analisadas por espectroscopia de infravermelho com transformada de Fourier (FTIR). A morfologia da superfície e do interior das esponjas foi caracterizada por microscopia eletrónica de varrimento (SEM). A adesão celular e internalização das células nas estruturas porosas foram visualizadas através de imagens de microscopia confocal. Os perfis citotoxidos dos biomateriais foram caracterizados por meio de ensaios de viabilidade celular, e os resultados obtidos confirmaram a sua biocompatibilidade. A actividade antimicrobiana dos biomateriais foi também avaliada e os resultados mostraram que as esponjas inibem o crescimento na sua superfície, do microrganismo mais comum das

infecções de pele (*Staphylococcus aureus*). As estruturas porosas têm propriedades adequadas para melhorar o processo de cicatrização de feridas cutâneas.

Table of Contents

Chapter I- Introduction

Chapter II- Materials and methods

Chapter III- Results and discussion

Chapter IV- Coclusion

Chapter V- Bibliography

List of Figures

Chapter I – Introduction

Chapter III – Results and discussion

List of Tables

Chapter I – Introduction

Chapter III – Results and discussion

List of Abbreviations

CFU	Colony forming units
CLSM	Confocal laser scanning microscopy
COX	Cyclooxygenase
COX-1	Cyclooxygenase-1
COX-2	Cyclooxygenase-2
CO_2	Carbon dioxide
CS	Coated sponge
PCL	Poly (ε-caprolactone)
DD	Deacetylation degree
DEJ	Dermal-epidermal junction
DMEM-F12	Dulbecco's modified eagle's medium
DMSO	Dimethylsulfoxide
ECM	Extracellular matrix
EDTA	Ethylenediaminetetraacetic acid
EGF	Epidermal growth factor
EtOH	Ethanol
FBS	Fetal bovine serum
FGF	Fibroblast growth factor
FTIR	Fourier transform infrared spectroscopy
GAGs	Glycosaminoglycans
IL-1	Interleukin-1
IL-6	Interleukin-6
K-	Negative control
K+	Positive control
LMW	Low molecular weight
M	Membrane
MW	Molecular weight
MMW	Medium molecular weight
MTT	3-(4,5-Dimethyl-2-thiazolyl)-2,5-diphenyl-2H-tetrazolium bromide
NaOH	Sodium hydroxide
NHDF	Normal human dermal fibroblast
NSAIDs	Nonsteroidal anti-inflammatory drugs
PBS	Phosphate buffered saline solution
PDGF	Platelet derived growth factor
PEO	Poly (ethylene oxide)
PFA	Paraformaldehyde
PI	Propidium iodide
RGD	Arg-Gly-Asp
RT	Room temperature

SB	*Stratum basale*
SC	*Stratum Corneum*
SEM	Scanning electron microscopy
SG	*Stratum granulosum*
SL	*Stratum lucidum*
SS	*Stratum spinosum*
S	Sponge
TE	Tissue Engineering
TGF-β	Transforming growth factor-β
TNF-α	Tumour necrosis factor-α
TPP	Tripolyphosphate
VEGF	Vascular endothelial growth factor
WHS	Wound Healing Society
3D	Three-dimensional

Chapter I- Introduction

1. Introduction

Skin is the largest organ of the human body and it plays highly specialized functions like at as a protective barrier against external insults that comprise ultraviolet light radiation (1), chemicals and microorganisms. Skin is also involved in fluid homeostasis maintenance, thermoregulation, immune surveillance, sensory detection and self-healing (2).

Skin injuries have a high impact on the life quality of patients. Skin injuries are caused by burns, accidents, diseases, surgery, trauma and bruises. Due to the various functions of the skin, any loss of skin integrity may result in organism disorders and ultimately in a significant patient disability or even death (2, 3). Skin disruption often leads to an increase in fluid loss, infection, scarring, compromised immunity and change in body image (4). For a complete restoring of both skin structure and function, successful wound healing must occur. The healing process of adult skin is complex, requiring the collaborative efforts of cells as well as both extracellular and intracellular signals (5, 6). With the objective to solve the problems associated with re-establishment of the native structure of skin and also the mechanisms responsible for healing, different wound dressings have been developed so for to protect the wound from bacterial infection, dehydration and allow wound exudate absorption (6). Nowadays, skin substitutes have a high demand for clinical uses. Actually, they represent approximately 50 % of Tissue Engineering (TE) and regenerative medicine market revenues.

TE is emerging as an interdisciplinary field in biomedical engineering that integrates many concepts of science and engineering in order to design and develop biological substitutes that restore, maintain or improve organs functions and damaged tissues regeneration (2, 7). It has appeared as a solution to the a number of clinical problems that were not properly treated by the conventional therapeutics in which wound healing of chronic wounds is include (8). In a near future, TE purposes to produce a biodegradable wound dressing that promotes the re-establishment of skin's native structure (Epidermis, Dermis and skin appendages). Furthermore, these skin substitutes are expected to reduce costs and pain associated with wound healing (Lanza et al., 2007).

1.1 Skin

1.1.1 Functions and structure

Skin provides an essential protective barrier against external environment avoiding pathogens invasion. Morever, this organ is also responsible for several hemostatic/sensory functions that are vital to health, namely the regulation of temperature and the hydration state for the human body (9-11). In detail, the skin functions are:

- **Hydratation:** Avoids patient dehydration;

- **Protection:** Confers protection against harmful external agents (ultraviolet light, mechanical, chemical and thermal insults), and also disables microorganisms penetration;
- **Sensativity:** Skin has various sensory receptors, that allow to monitoring of body temperature, touch, pressure, vibration and pain;
- **Metabolic:** Subcutaneous adipose tissue constitutes a major energy reserve, mainly in the form of triglycerides. Epidermis is synthesizes vitamin D, which is responsible for the maintenance of calcium and phosphorus concentration in the blood;
- **Thermoregulation**: Body temperature regulation, in which hair and pores are present at the surface of the skin.

Skin is organized in three anatomical distinct layers known as Epidermis, Dermis and Hypodermis (Figure 1). Between Epidermis and Dermis is a Dermal–epidermal junction (DEJ) that provides mechanical support for the Epidermis and acts as a partial barrier against larger molecules (10).

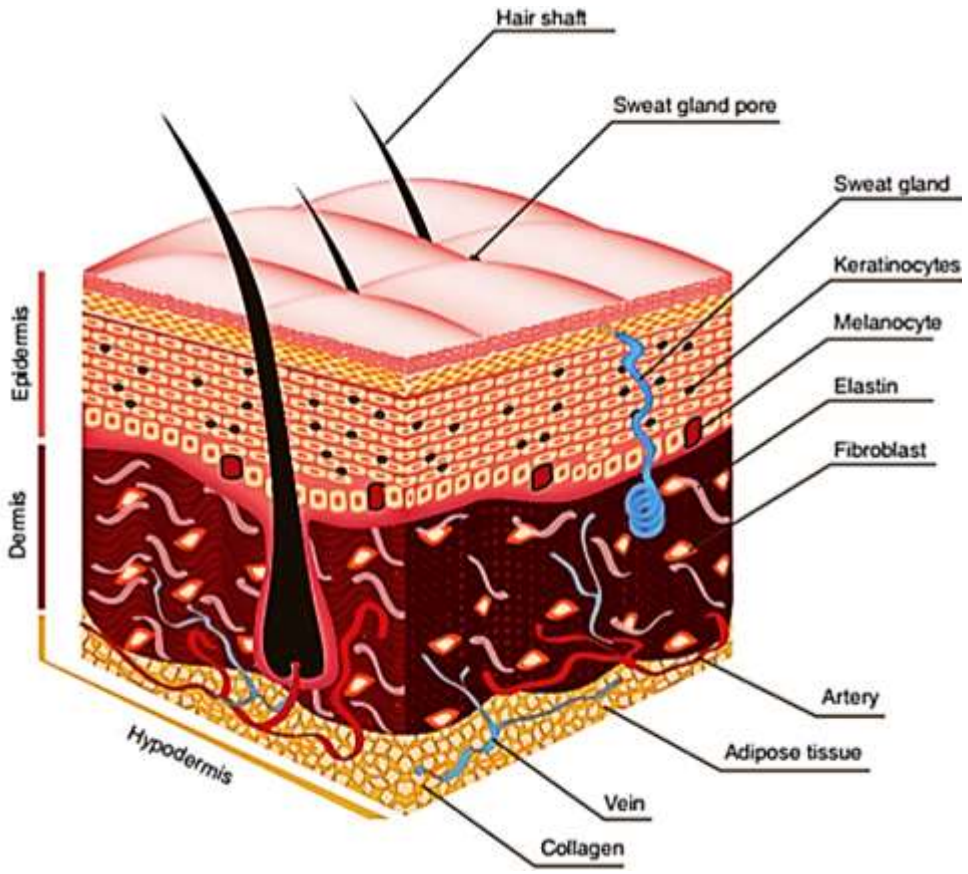

Figure 1: Structure of the human skin. Adapted from (12).

In the three layers of skin there are skin appendages such as, nails, hair follicles, sweat and sebaceous glands, nerves, lymphatic and blood vessels (13, 14).

1.1.1.1 Epidermis

Epidermis is the outermost layer of the skin, acting as a physical barrier against the external environment, preventing the water loss and infections (13). This layer is mainly constituted by keratinocytes (80 % of cellular elements), pigment-producing cells (melanocytes) and specialized dendritic Langerhans cells that have an essential role in the skin immune defense system (15, 16).

The Epidermis comprises 4-5 sublayers (17): *stratum basale (SB), spinosum (SS), granulosum (SG), lucidum (SL) and corneum (SC)*, as can be observed Figure 2.

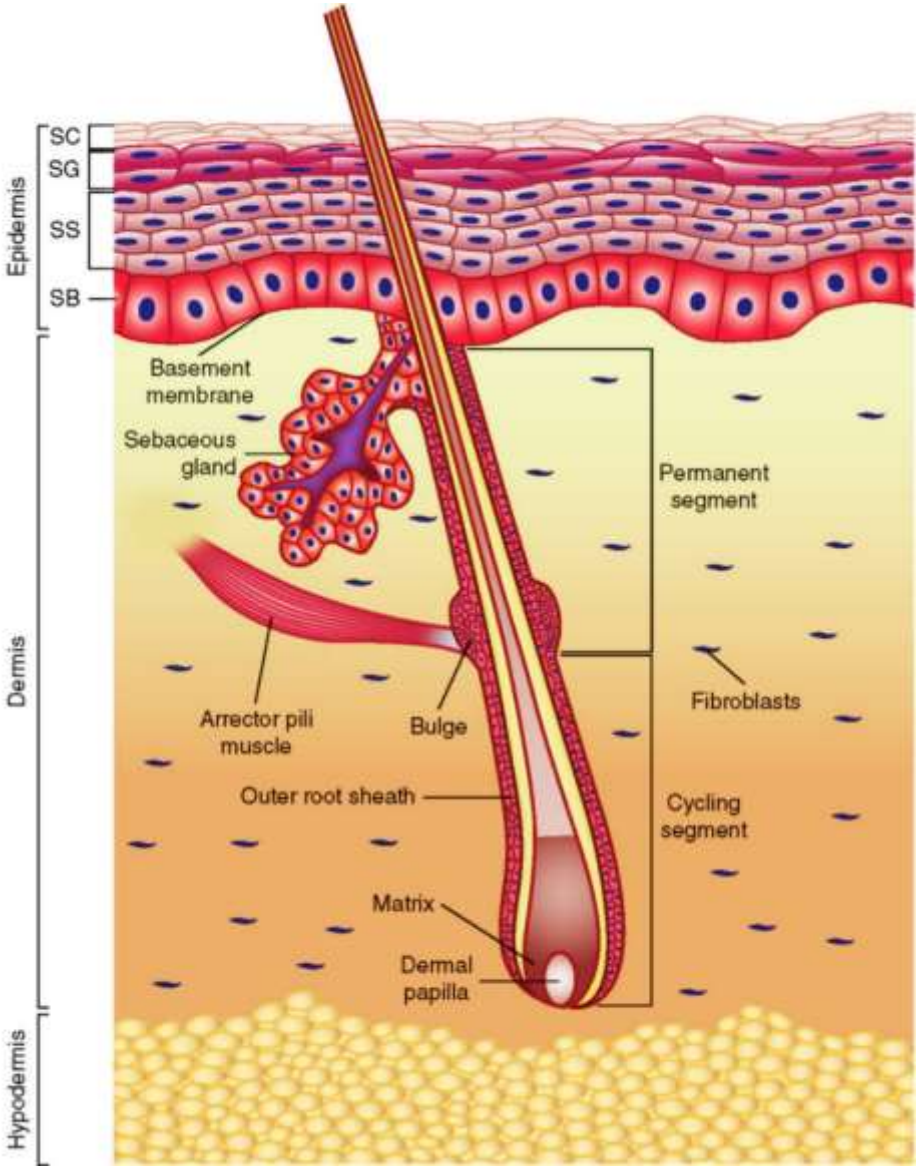

Figure 2: Representation of skin layered organization. Skin is composed of three layers: Epidermis, Dermis and Hypodermis. Epidermis is a stratified squamous epithelium that is divided into four layers, starting with the outermost layer: *stratum corneum (SC), stratum granulosum (SG), stratum spinosum (SS), and stratum basale (SB)*. Adapted from (18).

The *SB* is comprised mostly by keratinocytes that are in constant division. They are responsible for the continuous self-renewel of Epidermis. The *SS* also contains keratinocytes that are involved in the process of growth and early keratin synthesis (13, 14). The *SG* is characterized by the presence of intracellular granules that are involved in the process of keratinization (19-21). The *SL* represents 3–4 layers of dead and flat cells. This sub-layer is only found in the skin of palms and soles (13, 14). The final result of keratinocyte maturation is found in the *SC* (Figure 2), which is formed by completely differentiated dead keratinocytes (corneocytes). The resulting structure provides the physical barrier and prevent water loss of the human skin (13, 14, 22).

The Epidermis is bound tightly to the underlying Dermis through the basement membrane at the DEJ. The basement membrane can be divided into *lamina lucida* (the layer closer to the Epidermis that is made of laminin, entactins and dystroglycans) and *lamina densa* (a sheet-like structure composed mainly by collagen type IV). The whole basement membrane is involved in the mechanical stabilization of the Epidermis (14, 23, 24). Moreover, the basement membrane determines the polarity of the Epidermis and provides a barrier against Epidermal migration, which prevents the direct contact of Epidermal cells with the Dermis (23, 24)

1.1.1.2 Dermis

Dermis lies below the Epidermis and constitutes the main part of the skin (13). Dermis is composed by a high number of fibroblast cells that produce collagen type I and III, elastin and glycosaminoglycans (GAGs). These proteins are the main constituents of the extracellular matrix (ECM) and are responsible for the support and elasticity of the skin (14). Additionally, Dermis confers support to the vascular and lymphatic vessels and nerve bundles (Figure 2) (17, 25).

Dermis is divided in papillary and reticular layers. The superficial papillary Dermis is composed by thin fibers that are loosely arranged and contains blood vessels that supply the Epidermis with nutrients, remove waste products and help in body temperature regulation. The deeper reticular Dermis accounts for 80 % of Dermis and is composed by dense collagen and elastic fiber matrix, conferring strength and flexibility to the skin (17, 24)

1.1.1.3 Hypodermis

The Hypodermis, located below the Dermis, is also known by subcutaneous tissue, is mainly composed by fat and connective tissue (15, 16). This layer is highly vascularized, providing blood vessels and nerves to the skin and also allowing its connection to the underlying bones and muscles. Furthermore, it also contribute for the thermoregulatory and mechanical properties of the skin (12, 16).

1.1.1.4 Skin appendages

Skin has a variety of appendages, like, sweat and sebaceous glands, hairs folicules, nails and nerves. The sweat glands, secrete a watery fluid onto the skin surface, by the process of exocrine secretion. These glands play on important role in the thermoregulatory mechanism in humans (26). The main function of the sebaceous glands is to secrete sebum to moisturize the skin and hair and even the hair follicles, which are a source of proliferation of keratinocytes during epithelialization. Hair follicles also play an important role in the wound healing, once the Epidermal basal layer constitutes the outer cell layer of these structures and it has been shown that such basal cells, present in hair follicles, can move out and repopulate the Epidermis after healing. Nails confer protection to the distal phalanx and the fingertip (14). Moreover, skin contains a variety of nerve endings that sense heat and cold, touch, pressure, vibration and tissue injury. All cutaneous nerves have their cell bodies in the dorsal root ganglia, and both myelinated and non-myelinated fibers are found. Free sensory nerve endings lie in the Dermis where they detect pain, itch and temperature. Specialised corpuscular receptors also lie in the Dermis allowing sensations of touch (perceived by Meissner's corpuscles) pressure and vibration (by Pacinian corpuscles).

1.2 Skin wounds

Skin wounds affect millions of people worldwide, being one of the major issues of modern health care (5, 27). According to the Wound Healing Society (WHS), a skin wound can be described as a "disruption of normal anatomic structure and function" of skin, resulting from physical or thermal damage, medical procedures or physiological conditions (28).
Skin wounds can be classified in acute or cronic:

Acute wounds:

Acute wounds are usually characterized by a complete healing, with a minimal scar formation. The primary causes of acute wounds include mechanical injuries due to external factors, such as abrasions and tears that are caused by frictional contact between the skin and hard surfaces. Other examples of mechanical injuries include penetrating wounds caused by knives, gun shots or surgical procedures. Burns and chemical injuries (caused by radiation, electricity, corrosive chemicals and thermal sources) are another category of acute wounds (28). Acute wounds heal through a normal, orderly, and timely reparative process that results in a sustained restoration of the anatomic and functional integrity of this organ (28, 29).

Chronic wounds:

Chronic wounds are characterized by their slow healing (28). These type of wounds are commonly affected by several factors, such as the absence of clot formation (which reduce the levels of active/vital growth factors in the wound environment) and bacterial colonization that triggers a high immune response for removing the debris, leading to healing time (30, 31).

Chronic wounds usually occur in individuals who have underlying comorbidities, including peripheral blood vascular disease, obesity, diabetes, chronic steroid use, or other chronic diseases that impair tissue healing (30, 32). These wounds involve a large surface area and have a high incidence in general population, featuring an enormous medical and economic impact (33). Pressure, venous insufficiency, diabetic foot ulcers and ischemic wounds are the most prevalent types of chronic wounds (28, 33).

Additionally, skin wound can also be classified accordingly for the with the depth of injury and the number of layers affected: superficial, superficial partial-thickness, deep partial-thickness and full-thickness wound (28, 34):

Superficial wound:

Results from sunburns, light scalds and abrasions. In this type of wounds only the Epidermis is affected and they are characterized by erythema and minor pain. Such injuries do not require specific surgical treatment, since it regenerates without scaring occurs (34).

Superficial partial-thickness wound:

Affects Epidermis and superficial parts of the Dermis. Epidermal blistering and severe pain characterizes this type of injury, especially in the case of thermal trauma. The blood vessel, sweat glands and hair follicles are affected. The cells (keratinocytes) migrate towards each other from the basal layer to surround the wound. The healing occurs purely by epithelialization (28, 34).

Deep partial-thickness wound:

Injuries that involve great Dermal damage take long period to heal. Scaring is more pronounced for depth injuries, as well as the fibroplasia that is more intense, when compared with superficial partial-thickness wounds (5, 34, 35).

Full-thickness wound:

This type of wounds are characterized by a complete destruction of the skin appendages. The healing process involves contraction, and the epithelialization process occurs only from the edge of the wound. All full-thickness skin wounds are more than 1 cm in diameter and require skin grafting, as they cannot epithelialize on their own and may lead to extensive scarring, leading to limitations in joint mobility and severe cosmetic deformities for the patient (5, 34, 35).

1.2.1 Skin burns

Skin burns result from physical, chemical or thermal damages. The severity of the burn is determined by the patient condition (age and health) and it is usualy classified in degrees

depending on depth, position and size of the burned area (36, 37). Burns are usually divided in four degrees (Figure 3) (38, 39):

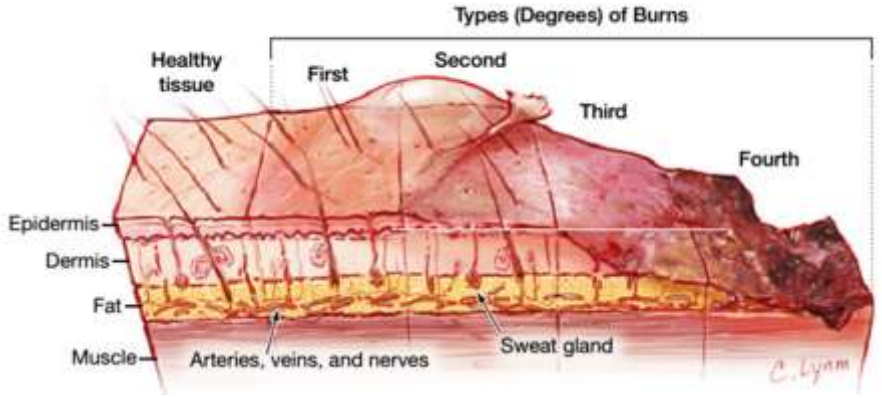

Figure 3: Representation of the different degrees (first, second, third and fourth) of skin burn severity. Adapted from (40).

First-degree (or superficial):

Burns affect only the top layer of the skin and are the least severe burns. It involves pain and edema formation. The skin usually takes several days to restore its structure, however the formation of scar does not occur. The superficial burns are healed in a period of 2 weeks (34, 40).

Second-degree (or partial-thickness):

Involves the Epidermis and part of the underlying Dermis destruction. Blisters are characteristic of in this type of burns (34, 40).

Third-degree (or full-thickness):

Affect all layers of skin, including the nerves. In these type of burns, skin is restored from the periphery involving the formation of granulation tissue and also scarring. Usually, in this type of burn the necrotic tissue resulting from the burn must be removed (34, 40).

Fourth-degree:

Burns extend into the muscle below the skin, including fat tissue, tendons, muscles and bones (40).

1.3 Wound healing

After, a lesion, skin integrity and function must be restored. The main goals of healing is to achieve a rapid wound closure and a functional and aesthetic scar (41). Although, if skin regeneration does not occurs properly significant disability or even death may occur (2, 3).

Skin wound healing is a complex process with an orchestrated cascade of events (e.g. coagulation, inflammation, phagocytosis, chemotaxis, mitogenesis, epithelialization and ECM proteins production) (4, 42), where different cellular elements (e.g. platelets, neutrophils, macrophages, keratinocytes and fibroblasts) and soluble factors (e.g. cytokines and growth factors) are involved.

Skin healing process can be divided into four overlapping phases: (i) haemostasis, (ii) inflammation, (iii) cell migration and proliferation and (iv) remodeling (43) as displayed in Figure 4.

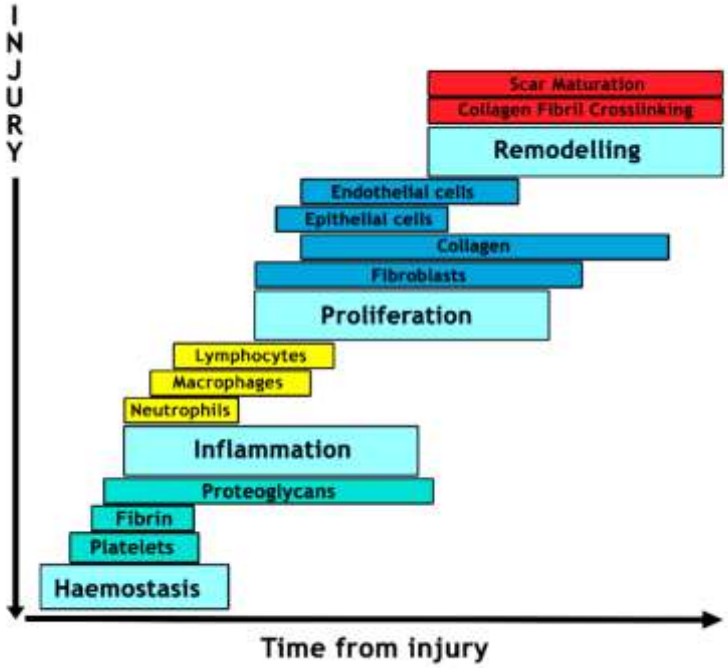

Figure 4: Representation of the phases of the wound healing. This process involves diferente types of cells and various phases. Phase I - Haemostasis which is characterized by coagulation and platelet activation; Phase II - Inflammatory phase where the cells of the immune system are recruited to injury site; Phase III - Proliferation phase occur the formation of ECM, granulation tissue and also angiogenesis; Phase IV - Remodeling, where the formation and maturation of the scar occurs.

1.3.1 Phases of wound healing

1.3.1.1 Haemostasis

After a tissue injury, the disruption of blood vessels is responsible for the extravasation of blood constituents (5, 35, 44). Bleeding typically occurs when the skin is injured and it allows the removal of bacteria and/or antigens from the wound. In addition, bleeding triggers platelet aggregation, fibrin clot formation and activates the coagulation cascade in order to prevent ongoing fluid losses. Haemostasis is achieved initially by the formation of a platelet plug,

followed by the formation of a fibrin matrix that allows cells infiltration. The clot dries to form a scab and provides strength and support to the injured tissue (Figure 5) (28, 45).

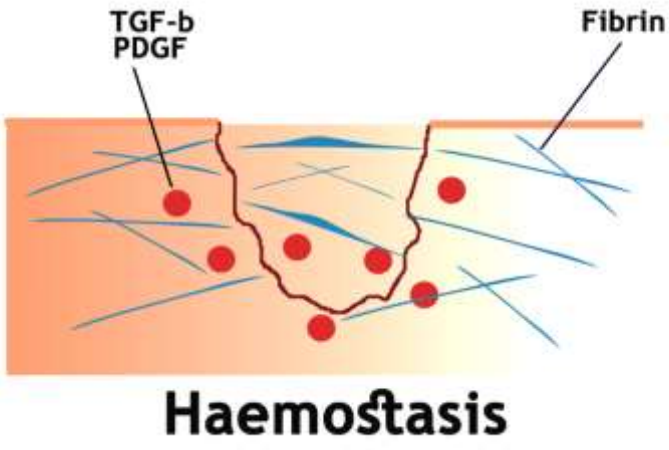

Figure 5: Representation of first phase of wound healing process: Haemostasis. The red balls represent the platelets releasing several factors, including platelet derived growth factor (PDGF) and transforming growth factor ß (TGF-ß).

The cytoplasm of platelets contains α-granules filled with growth factors and cytokines, such as PDGF, TGF-ß, epidermal growth factor (EGF) and insulin-like growth factors. They also contain dense bodies that store vasoactive amines, like serotonin, which increase the microvascular permeability (35). There is an invasion of inflammatory cells such as leukocytes, macrophages and neutrophils of the wound site. These cells and platelets release cytokines and growth factors in order to activate the inflammatory process (35).

1.3.1.2 Inflammation

The inflammatory phase begins almost simultaneously with haemostasis, sometimes from within a few minutes of injury to 24 hours, and lasts for about 3 days. This phase can be divided into two stages (early and late inflammatory phases) depending either on the time and duration of the response and the type of inflammatory cells involved (35).

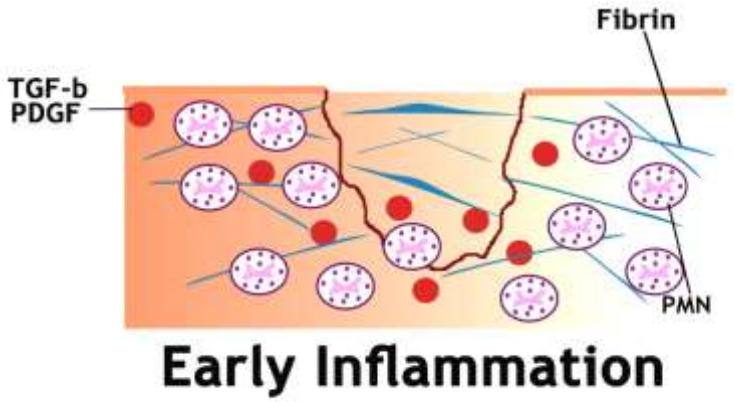

Figure 6: Representation of early inflammatory phase. The red balls represent the platelets that release several factors, including PDGF and TGF-β, which attract PMNs to the wound, signalling the beginning of inflammation. The blue traces represents fibrin.

In the early inflammatory phase the activation of coagulation and complement system leads to the release of chemoattractants that recruit neutrophils into the wound site (Figure 6) (46). Then, the degranulation of platelets occurs. Moreover, once at the wound site, neutrophils perform their function of killing and phagocyte bacteria and damaged matrix proteins within the wound bed. The role that neutrophils play is crucial within the first days after injury, due to their ability to perform phagocytosis and also secrete proteases, that are involved in killing bacteria and also on degrade the necrotic tissue (42).

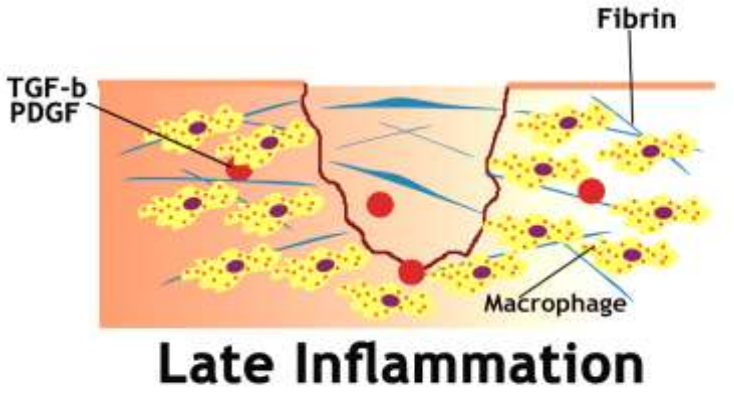

Figure 7: Representation of late inflammatory phase. The yellow clots represents the aggregate of macrophages with the PMNs, which are responsible for removing the debris from the wound, release growth factors and begin to reorganize the ECM. The red balls represent the platelets releasing several factors, including PDGF and TGF-β and traces of fibrin.

After 2-3 days in the late inflammatory phase, monocytes appear in the wound area and differentiate into macrophages (5). These macrophages are the most essential inflammatory cells involved in the normal healing response, as can be observed in Figure 7. Once activated

they perform phagocytosis of pathogens and of cell debris as well as the secretion of chemokines, inflammatory cytokines (interleukin-6 (IL-6), tumour necrosis factor (TNF-α) that stimulate the re-epithelialization) and growth factors such as: EGF (that stimulates the re-epithelialization), TGF-β, fibroblast growth factor (FGF), PDGF (which promote cell proliferation and the synthesis of ECM molecules by resident skin cells) and vascular endothelial growth factor (VEGF) (that stimulates the angiogenesis and granulation) (5). Macrophages act as phagocytic cells and secrete growth factors that are responsible for the proliferation of endothelial and smooth muscle cells and also for the production of ECM components by fibroblasts. They also involved in the release of enzymes that help to debride the wound (42). The presence of macrophages at the wound site is a marker that the inflammatory phase is finishing and the proliferative phase is beginning.

1.3.1.3 Cell migration and proliferation

The migration phase is the final stage of visible wound healing process (Figure 8). This phase involves the migration of keratinocytes, fibroblasts and endothelial cells to the wound site in order to replace the damaged tissue (47). In this phase, the wound is filled with granulation tissue. The endothelial cells of the adjacent venules initiate the angiogenesis process. These cells also synthesize remodelling enzymes that perform the breakdown of the ECM and thus create defects into which new capillary vessels will form a network and restore the vasculature (5, 28, 35, 39, 44).

The proliferative phase starts three days after injury and lasts for about 2 weeks (35, 47). It is characterized by fibroblasts cells migration and by the deposition of newly synthesized ECM and formation of granulation tissue (35, 48). With progression of the proliferative phase, the provisional fibrin/fibronectin matrix is replaced by the newly formed granulation tissue (48). Epithelialization of the wound represents the final stage of the proliferative phase (35).

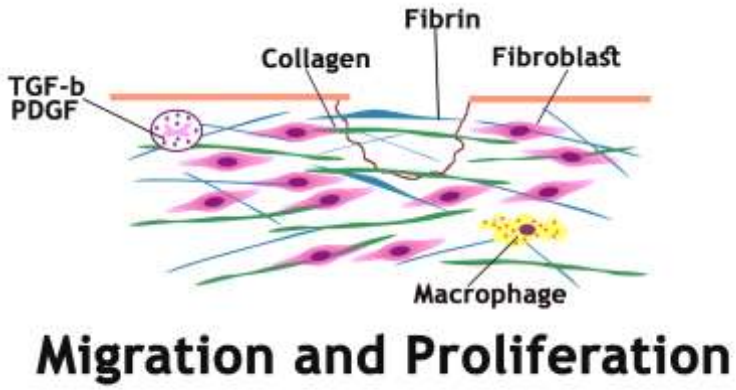

Figure 8: Representation of migration and proliferation phase. The proliferation phase begins when fibroblasts are recruited to the wound site through the release of growth factors by inflammatory cells. Then fibroblasts start the synthesis of collagen.

Migration of fibroblasts:

Fibroblasts appear at the wound site after 2–4 days and endothelial cells come about one day later (5). Following injury, fibroblasts are attracted to the wound by a several growth factors, including PDGF and TGF- ß. After that, fibroblasts proliferate and produce the matrix proteins: fibronectin, hyaluronan, collagen and proteoglycans. These components are involved in the production of a new ECM, which supports the migration and proliferation of cells (35, 47).

Production of the new ECM:

The ECM is composed by a network of structural proteins (collagens and elastin) and by an interstitial matrix composed by the adhesive glycoproteins (fibronectin, laminin and thrombospodin) embedded in a proteoglycan and GAGs (5, 49). In wound healing, PDGF, FGF, TGF-ß, interleukin-1 (IL-1), TNF induce collagen synthesis during the proliferative and remodeling phases (35, 50).

Formation of the granulation tissue:

After 3–5 days, the development of the granulation tissue occurs, which is characterized by a high density of fibroblasts, granulocytes, macrophages, capillaries and loosely organized collagen bundles (5, 35). Angiogenesis and neovascularization are also processes that occur in to this phase. (5, 35, 42, 49).

Epithelialization:

Within a few hours often skin injury, a single layer of Epidermal cells migrate, from the wound edges, to form a covering over the damaged area. Along this process, a new basement membrane is produced and, thereafter, the growth and differentiation of epithelial cells allows the re-establishment of the stratified epithelium. At the end of this phase the myofibroblasts are responsible for wound contraction, bringing the edges together. The appearance of myofibroblasts corresponds to the initiation of connective-tissue compaction and the contraction of wound (5, 35).

1.3.4 Remodelling (maturation)

Remodelling is the last phase (Figure 9) of the wound healing and occurs from day 21 to up to 1 year after injury. At this stage, the majority of endothelial cells, macrophages and myofibroblasts undergo apoptosis or exit from the wound, leaving a mass that contains few cells and consists mainly of collagen and other ECM proteins (5).

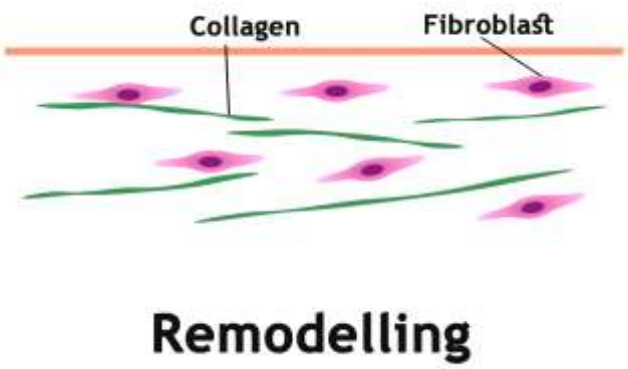

Figure 9: Representation of the remodeling phase. The green represents collagen and the purple fibroblasts.

This stage involves the formation of cellular connective tissue and strengthening of the new epithelium. There is a continuous synthesis and breakdown of collagen as well as the remodeling of ECM. Such determines the nature of the final scar (Enoch and Leaper, 2008). Most of the endothelial cells, macrophages and myofibroblasts undergo apoptosis or exit from the wound, leaving a mass that contains few cells and mostly collagen and other ECM proteins (42).
Probably, the interactions between the epithelial mesenchymal cells will remain to support the skin integrity and homeostasis. In addition, over 6–12 months, the collagen type III that was produced in the proliferative phase is now replaced by collagen type I. This process is performed by matrix metalloproteinases secreted by fibroblasts, macrophages and endothelial cells (5).
Finally, the angiogenic response decreases, the wound blood flow decreases and the acute wound metabolic activity slow down and stop. Subepidermal appendages such as hair follicles or sweat glands are not re-established after a serious injury (5, 42, 51).

1.3.2 Types of wound healing

In each healing process there are several mechanisms involved. The severity of the wound, number of skin layers affected and the occurrence or absence of bacterial infection allows us to classify the wound healing in different categories (5, 35):

Primary healing:

Occurs when a wound, created by laceration or surgical incision, causes only focal disruption of the continuity of the epithelial basement membrane and death of some cells of the underlying connective tissue. The wound is closed within 12-24 hours of its occurrence; In this type of healing, epithelial regeneration predominates over fibrosis (35, 44).

Delayed primary healing:

Occurs in a contaminated or poorly delineated wound. The closure is performed after the host defenses have helped to debride. After 3-4 days, phagocytic and inflammatory cells are recruited to the wound site to remove the contaminating bacteria. Collagen metabolism is usually unaffected and the wound retains its tensile strength (35, 44).

Secondary healing:

Occurs when the wound edges cannot be approximated, due to the extensive loss of soft tissue, caused by a major trauma like severe burns and some surgical procedures. This type of wound healing is common in patients with underlying co-morbidities such as vascular, diabetic and pressure ulcers. The wound is left open and thus more susceptible to infections. The epithelial cells are not capable to restore the skin original architecture, so there is ingrowth of granulation tissue from the wound margins, followed by accumulation of ECM with the laying down of collagen. Myofibroblasts, which have structural properties similar to that of fibroblast and smooth muscle cells, are thought to play a crucial role in the healing of this type of injuries. The secondary healing is slower and may lead to functional defects (35, 44).

Superficial healing:

It is observed in injuries such as superficial burns, split-thickness donor graft sites, and abrasions where the injury involves the epithelium and the superficial (papillary) part of the dermis. The basal layer of cells remains uninjured and the epithelial cells within the Dermal appendages, hair follicles, and sebaceous glands replicate to cover the exposed Dermis; the cells migrate towards each other from the basal layer to surround the wound. Healing occurs purely by epithelialization (35).

1.4 Tissue engineering

TE is a field that applies the principles of biology, engineering and medicine in order to develop the biological substitutes that restore, maintain or improve damaged tissues or organs functions (2). It appeared as a solution for a number of clinical problems that were not properly treated with the use of permanent replacement devices (8).

The underlying concept of TE is to isolate cells from a patient and then produced to their expansion and incorporation in a 3D matrix. The resulting TE construct is then grafted back into the same patient to function as a replacement tissue. In this approach, a highly porous artificial ECM, or scaffold, is required to accommodate mammalian cells and guide their growth in three dimensions.

Major advances in materials science and engineering have contributed for the continuous development of TE and regenerative medicine (7, 52, 53). Nowadays, the tissue engennering is a discipline already applied in a significant number of medical procedures for skin (54), liver (55), pancreas (56), intestines (57), esophagus (58), nerves (59), cartilage (60), bone (61), and tendon (62) replacement.

1.4.1 Tissue engineering applied to wound healing

Autografts, allografts and xenografts are the most used therapeutic approachs for skin regeneration. Autografts are obtained from the patient and present a higher healing success rate. However, they have a limited supply and its obtention is associated to morbidity in the donor site (63, 64). Allograft skin is harvested from organisms of the same specie. The use of allograft skin is limited since there is a great risk of disease transmission, eventual immune rejection and other limitatiors associated with its storage (65). The demand for tissues and organs seriously exceeds the supply, creating a substantial waiting list. Moreover, the immune system tends to reject the foreign tissue or organ (14). Xenograft skin is harvested from a different species and the majority of xenograft tissues are rejected by the immune response of the host, that may be caused upon the implantation process, thus leading to a high failure rate (66-68).

In order to overcome the drawbacks associated with the use autografts, allografts and xenografts, different studies have been performed in the area of TE to developed new skin substitutes that can contribute to reduce the mortality and morbidity caused by scarring, changes in pigmentation, reduce the number of surgical procedures and hospitalization period (69).

In the development of materials aimed to produce new skin substitutes it is necessary to take into account three major requirements: the safety of the patient, the clinical efficacy and the convenience of handling and application. Nowadays, skin substitutes are highly porous and some of them can accommodate skin cells and guide their growth in three dimensions (70).

1.4.1.1 Comercial available skin substitutes

Different skin substitutes are already applied in the clinic. Skin substitutes are a heterogeneous group of wound coverage materials that aid in wound closure and help in the reestablishment of the functions of the skin (28, 71, 72). Most of the bioengineered skin devices currently available consist on a combination of sheets of biomaterial matrix (e.g. collagen, hyaluronic acid) containing cultured cells (73-75). Several types of temporary dressings have been designed to provide a bacterial barrier to decrease pain and contribute to an adequate environment for epithelial regeneration.

Wound dressings have been widely used due to their relative low cost, ease use, and effectiveness to clean and protect the wound from the external environment. They act as physical barriers that protect the wound from microorganism invasion and promote moisture environment and allow gases exchanges.

The commercial bioengineered skin equivalent products are classified accordingly to the following parameters (2, 74-76):

A. **Type of the biomaterial used for their production:**
    a. **Biological** – e.g. Epicel;
    b. **Synthetic** – e.g. MySkin.

B. **Composition regarding the cellular components:**
    a. **Cellular –** e.g. Dermagraft;
    b. **Acellular –** e.g. Integra Dermal regeneration.

C. **Duration:**
    a. **Temporary** – e.g. Dermagraft;
    b. **Semi-permanent** – e.g. Integra Dermal regeneration;
    c. **Permanent** – e.g. Epicel.

D. **Layer of skin that skin substitutes are able to replace:**

Epidermal substitutes - keratinocytes are isolated from a donor and then are cultured *in vitro* in order to obtain the necessary number of keratinocytes for therapeutic purposes. Several Epidermal skin substitutes are already commercially available:

a) **Epicel ™:** is a permanent substitute, which is composed by the *in vitro* culture of autologous keratinocytes (confluent cellular sheets) (34, 77).

b) **EpiDex ™:** *in vitro* cultured autologous keratinocytes collected from hair bulbs (confluent cellular sheets). It is a permanent substitute (17, 77).

c) **MySkin ™:** *in vitro* cultured autologous keratinocytes (subconfluent cellular sheets) which are grown on a silicone support layer with a specially formulated surface coating (34, 77).

Dermal substitutes - Dermal substitutes are usually acellular, based on allogeneic, xenogeneic or synthetic materials (78). Dermal skin replacements present advantages, such as reduced costs, easier manufacture and rigorous quality control. They also add mechanical stability and prevent the wound from contracting (2, 34). However, they can be rejected by the host and be involved in diseases transmission (15). The Dermal substitutes available in include:

a) **Dermagraft ™**: is composed of polyglactin mesh seeded with living cultured neonatal fibroblasts. It is a temporary substitute (79).

b) **Alloderm** is a freeze-dried human acellular dermal matrix. This type of matrix is ready to be incorporated into the wound, and it does not any immunogenic response from the host due to absence of a cellular component (80);

c) **Integra®:** is composed by two layers: a porous layer of the skin made of bovine collagen type I and shark chondroitin-6-sulphate GAG that is bonded to a silicone pseudo-epidermis Integra®. It is indicated for the treatment of full thickness or deep partial thickness burns (17, 81).

Dermo-epidermal substitutes - These substitutes mimic the Epidermal and Dermal layers. These substitutes are more advanced than the Epidermal and Dermal ones, although they are the most expensive (82).

a) **Apligraf ™:** is composed by viable allogeneic neonatal fibroblasts grown in a bovine collagen type I gel matrix, combined with viable allogeneic neonatal keratinocytes. It supplies ECM components to the wound, as well as cytokines and growth factors (77, 81).

b) **PermaDerm ™:** is composed by an Allogenic matrix with bovine collagen. It is a permanent substitute (77).

c) **OrCell ™:** is a TE skin construct that includes cultured allogenic fibroblasts and keratinocytes from the same neonatal foreskin. Fibroblasts are seeded into a bovine type I collagen sponge (77).

1.5 Polymeric sponges for skin regeneration

Despite the existence of various skin substitutes, none of them is capable of completely replicate the anatomy, physiology, biological stability or aesthetic nature of native skin (15).
In addition, they are expensive, require frequent replacement, making the patient susceptible to subsequent secondary bacterial infections. Having this knowledge in mind, there is a huge demand for developing alternative strategies for treating burns or other skin lesions. Researchers from the area of TE have develop new Dermis and Epidermis substitutes using natural or synthetic matrices (83), in order to promote a more rapid and improved healing as well as a reduced scarring (2).
Based on the properties that skin substitutes must have, porous scaffolds emerged as a promising alternative to be used as skin substitutes.
Sponges are three-dimensional (3D) matrices that act as temporary templates for cell adhesion and proliferation, while providing mechanical support, until the new skin tissue is formed at

the affected area. Polymeric sponges are potential scaffolds for skin regeneration since they satisfy several requirements (84, 85):

a) Protect the wound from fluid and proteins loss;
b) Easy to handle and apply at the wound site;
c) Present controlled degradation;
d) Enable exudates absorption;
e) Minimize scar formation;
f) Large surface area that enables cell adhesion, growth and differenciation;
g) Great porosity that allows cell infiltration, diffusion of nutirents and gases exchange;
h) A surface can be easily modified (e.g. with the use of coatings);
i) Can be produced using various techniques;
j) Biocompatible: ability of a biomaterial to perform its desired function, without eliciting any undesirable local or systemic effects in the recipient or beneficiary of that therapy (10);
k) Biodegradable: The by-products of their degradation must be non-toxic and able to exit from the body without interference with other organs. In order to allow degradation at a rate compatible with tissue formation, an inflammatory response combined with controlled infusion of cells such as macrophages is required;
l) Active biomoluces (e.g. growth factors, cell-surface interactive peptides, drugs) can be easily incorporated to the sponge matrix that will facilitate skin regeneration, to stimulate cellular attachment, migration and proliferation.

Based on these properties the development of sponges for skin regeneration may have a huge potential for skin healing.

1.5.1 Methods and techniques used for sponge production

Differents methods have been used for the development of sponges for TE, including the supercritical fluid technology, porogen leaching, freeze drying, scaffold templating (see Table 1, for further details).

Supercritical fluid technology:

In this process, high pressures are used to dissolve the polymeric solution with or without a porogen. When a supercritical fluid such as carbon dioxide is used as a nonsolvent, the simple tuning of the processing conditions (pressure and temperature) can tailor the final structure of the sponges. Also, any subsequent drying step is avoided, as the obtained porous structure is a dry product free of any residual solvent (86, 87).

Porogen leaching:

Porogen leaching allows the control of pore size and porosity of sponges, allowing the obtention of scaffolds with a more homogeneous pore morphology (86). Porous structures from polymers such as PCL has been produced using this method (88).

Freeze drying:

The method is based on the formation of ice crystals that induce porosity through ice sublimation and desorption. The kinetics of the freezing stage controls the porosity and the interconnectivity of the foams (89). 3D structures with values of porosity up to 200 % (86) with different interconnectivities are commonly obtained by freeze-drying. The main difficulty associated with this process is to ensure structural stability and adequate mechanical properties of the porous constructs after subsequent hydration. This limitation hinders its use when the application involves conditions with mechanical stress, even at low-to-moderate levels.

Scaffold templating techniques:

Polymeric solutions may be injected into moulds to fabricate scaffolds with various shapes and sizes. Also, the mould template can be design to fabricate a macroporous scaffold (86).

Table 1: Technologies used for the production of 3D constructs. Adapted from (86).

Fabrication technology	Processing	Pore size (μm)	Porosity (%)	Advantage	Disadvantage
Supercritical fluid technology	Casting.	<50 and <450	<95	-	-
Porogen leaching	Casting.	30–300	20–50	3D scaffold.	Limited control of pore size and shape.
Freeze drying	Casting.	<200	<97	Easy processing; 3D Scaffold.	Limited control of porosity.
Templating	Casting and spinning.	30–200	<80	Cell incorporation.	Slow processing time.

1.5.2 Coating of sponges

Electrospinning has been recognized as the simplest technique to produce continuous nanofibers from diverse materials, including polymers (90).

Electrospinning is a process that comprise the application of a needle attached to a syringe filled with polymer solution, a grounded collector plate and a high voltage power supply connected between the capillary and the collector. The feeding rate of the polymer solution is usually controlled using a syringe pump. A charged polymer solution flowing out of the needle is accelerated towards the grounded collector by a strong electrostatic field (91, 92). This field causes the droplet to emerge from the needle to undergo deformation into a conical shape, known as the "Taylor cone". When a critical value is attained (the repulsive electrostatic force overcomes the surface tension) a fine jet of the solution emerges from the Taylor cone. The jet undergoes twisting instability and a characteristic whipping motion due to the charge-charge repulsion that occurs between the excess charges presented in the jet (Figure 10), and during this phase, the jet is drawn by at least two orders of magnitude, the solvent evaporates, and the dry fibers deposit onto the collector (91, 92).

The properties of the nanofiber mesh depending on fiber diameter, porosity characteristics of the solution and electrospinning equipment processing parameters. The smaller size of the individual fibers, the higher the surface area to volume ratios, which leads to an increase cell proliferation (93). The size, shape, individual fibers, the porosity of the web of fibers obtained and chemical compositions can be easily manipulated (94).

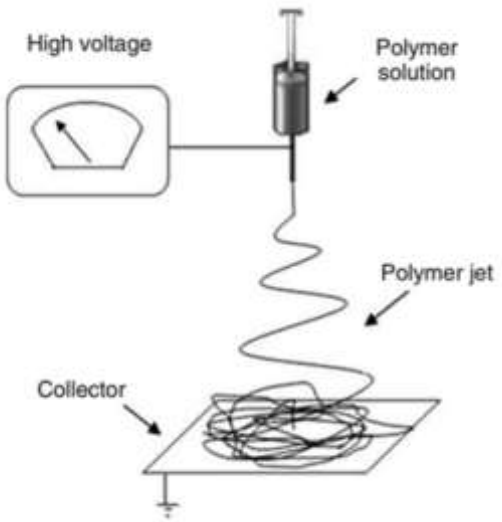

Figure 10: Schematic diagram of the electrospinning setup. Adapted from (25).

In biomedical applications the ultrafine fibrous scaffolds produced by electrospinning have been demonstrated to have suitable properties to promote the adhesion, proliferation and differentiation of several types of cells (94).

Moreover, electrospun fibers can be used to coat scaffolds aimed for tissue regeneration, namely skin regeneration. Several electrospun nanofibrous membranes a contribution of natural/synthetic materials have been already tested for skin regeneration, produced with natural materials or polymers. Electrospun nanofibers reproduce the native topographical features of the natural ECM, promoting the cell's natural functions (95, 96).

Most of the work performed in this field uses biodegradable synthetic polymers (such as PCL) to produce non-woven membranes for various TE or drug delivery applications (97).

Currently, a variety of natural polymeric-based membranes obtained from Chitin (98), Chitosan (99, 100), Alginate (100), Cellulose (101, 102), Hyaluronic acid (103), Gelatin (104, 105), Collagen (106) and their derivatives have been developed in order to satisfy the hight demand for new materials for the treatment of different wounds. These types of membranes may be composed of dense top layer and underlying porous sponge-like layer. The external layer protects the wound and serves as an artificial Epidermis, while the inner layer is designed for the drainage of wound exudates and attachment of wound tissues (107, 108).

1.5.3 Biomaterials used for sponges production

The first issue with regard to the development of a scaffold for skin TE is the choice of suitable material. Natural polymers can mimic many features of ECM and thus can guide the migration, growth and organization of cells during the wound healing process (109, 110).

These natural polymers include polysaccharides, like Chitosan or proteins-based polymers (Collagen, Fibrin gels, Silk, and Gelatin). Despite their low mechanical strength, these natural

polymers have high hydrophilicity, low immune reaction and promote cell adhesion and proliferation (111).

1.5.3.1 Chitosan

Chitosan is a cationic polysaccharide composed of copolymers of ß (1→4)-glucosamine and N-acetyl-D-glucosamine (Figure 11). It presents important characteristics for biomedical applications, such as, biocompatibility, biodegradability, hydrophilicity, hemostatic activity, nonantigenicity, anti-microbial activity and promote wound healing (108, 112). In addition, Chitosan is very abundant, has a low production cost and is environmental friendly.

Chitosan has been applied in the area of TE for a wide variety of applications, like skin regeneration. It induces a faster wound healing and produce smoother scarring possibly due to an enhanced vascularization (113).

Another important property of Chitosan is its antibacterial activity for different strains, such as *Enterobacter aerogenes, Salmonellas Typhimurium, Staphylococcus aureus and Escherichia coli* (84, 114, 115). Due to this bactericidal activity Chitosan has been blended with other polymers (71, 116). Its antimicrobial activity may result from the electrostatic interactions between the positively charged Chitosan with negatively charged molecules at the cell surface, which affects cell permeability (71). This electrostatic attraction promotes cells' adhesion, proliferation and differentiation (116, 117).

Different studies reported the use of Chitosan for the production of skin substitutes, due to its properties that stimulate haemostasis and fibroblast to synthetize collagen, improving the tissue regeneration (118, 119). *In vivo*, this polymer stimulates the adhesion of fibroblasts, promoting keratinocytes proliferation and modulate the migration of neutrophils and macrophages, which in turn, modifies the repairing processes such as fibroplasias and reepithelialisation (66, 71).

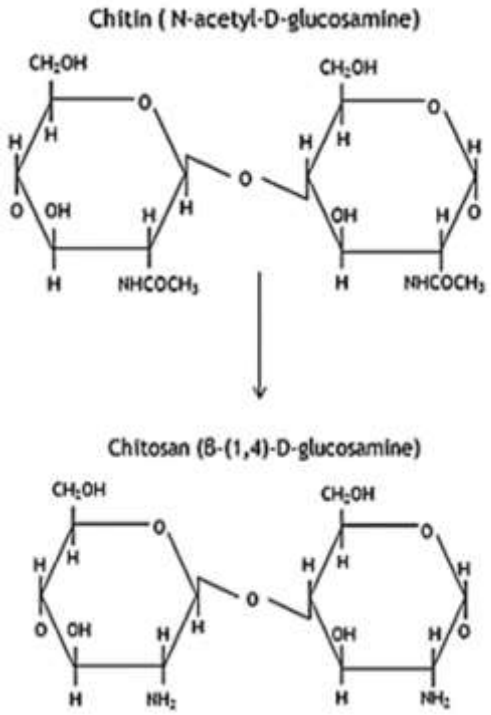

Figure 11: Chemical structure of Chitosan. Adapted from (120, 121).

The deacetylation degree (DD) of commercial available Chitosan is usually between 70 % and 95 %. The different DD are defined in terms of the percentage of primary amino groups in the polymeric matrix (122). Chitosan with higher DD presents a greater number of free amino groups (71). Chitosan is degraded *in vivo*, through enzymatic hydrolysis. Lysozyme is the primary enzyme responsible for the in vivo degradation of Chitosan.

1.5.3.2 Gelatin

Gelatin is produced by partial hydrolysis of collagen extracted from the boiled bones, connective tissues, organs and some intestines of animals. Gelatin is colorless, brittle (when dry) and a flavorless solid substance. It is commonly used as a gelling agent in food and pharmaceuticals. Gelatin is biodegradable, biocompatible and has low antigenicity (122). Although, it obtained from collagen, it still retains some its properties, such as tripeptide Arg-Gly-Asp (RGD) sequence, that promote cell adhesion, differentiation and proliferation (123). Furthermor it also has a low cost and low immunogenicity. It is soluble at physiological pH and at 40 °C. The large number of amino, carboxyl and hydroxyl groups, allows Gelatin chemical modification, increasing its versatility (Figure 12). Gelatin has been investigated for the production of matrices for skin regeneration (sponge or film) that can promote the epithelialization and granulation tissue formation (124).

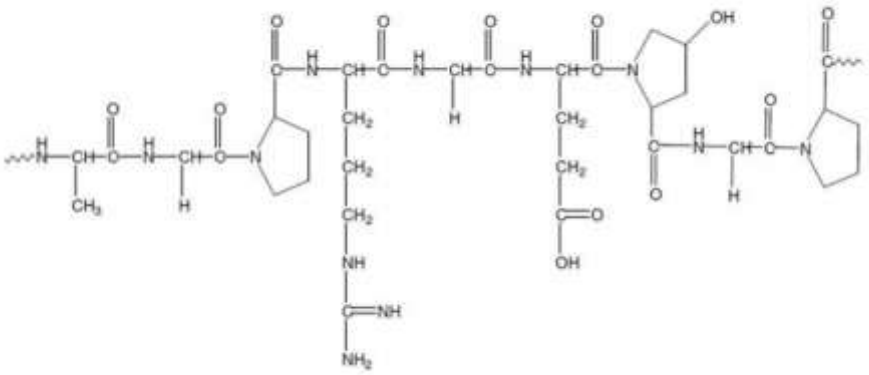

Figure 12: Representation of Gelatin structure. Adapted from (125).

1.5.3.3 Poly (ethylene oxide)

PEO is a unique class of water-soluble biodegradable biopolymer (Figure 13). Due to its excellent biocompatibility, biodegradability and potential to be used in biomedical applications has attracted a great attention from both the industrial and scientific areas (113, 126). PEO is also used to reduce the viscosity of Chitosan solution, so that the solution is extruded at high polymer concentrations.

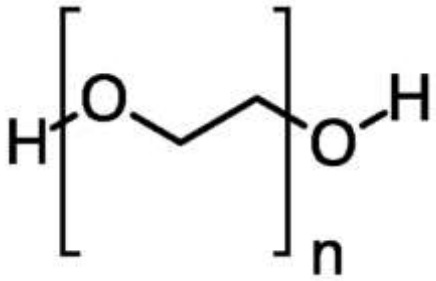

Figure 13: Structure chemical of PEO.

1.5.3.4 Poly (ε-caprolactone)

PCL (Figure 14) is a polyester that exhibits good mechanical properties. It a semi-crystalline material. However, due to its hydrophobic character, contains very few cell recognition sites and has a slow degradation rate. This polymer is used for various biomedical applications such as sutures, drug delivery systems and scaffolds in TE, due to its soft- and hard-tissue compatible properties (72).

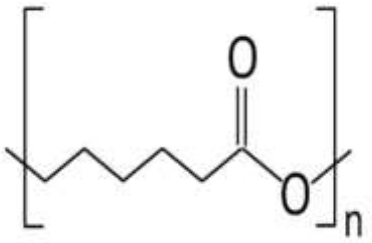

Figure 14: Structure chemical of PCL.

1.5.4. Incorporation of anti-inflammatory drugs in sponges for skin regeneration

Nonsteroidal anti-inflammatory drugs (NSAIDs) are the most commonly used drugs to treat inflammatory diseases, since they are effective in the management of pain, fever, redness, edema that occur as a consequence of inflammatory mediator release (127, 128). Different studies have shown that both therapeutic and side effects of NSAIDs are dependent of cyclooxygenase (COX) inhibition. COX isoforms have been named constitutive cyclooxygenase-1 (COX-1) and inducible cyclooxygenase-2 (COX-2). COX-1 (such as indomethacin, naproxen, Ibuprofen) catalyzes the formation of cytoprotective prostaglandins in thrombocytes, vascular endothelium, stomach mucosa, kidneys, pancreas, langerhans islets, seminal vesicles and brain (128, 129). Induction of COX-2 by various growth factors, proinflammatory agents, endotoxins, mitogens and tumor agentes (130, 131) indicates that this isoform may have a role in occurence of pathological processes, such as inflammation (132, 133). As a result of studies focused on reduction of the adverse effects of NSAIDs, selective COX-2 inhibitors, such as celecoxib and rofecoxib, have been developed. Today, it is a well-known hypothesis in medicine that COX-1 is constitutive and cytoprotective, while COX-2 is an inducible enzyme in the inflamed tissues (Figure 15).

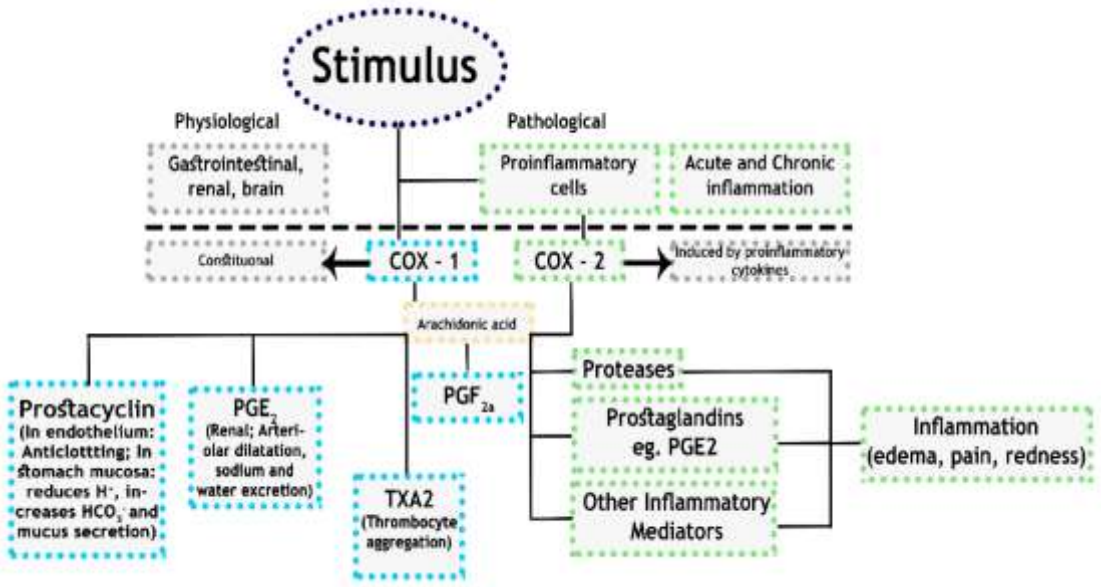

Figure 15: Mechanism of action of the COX-1 and COX-2 in the human body.

NSAID in general in particular Ibuprofen, have been shown to have benefic effects on various acute conditions ranging from sepsis, traumatic induced pulmonary damage and wound healing.

1.5.4.1 Action of Ibuprofen in the wound healing process

Ibuprofen has been shown to have benefic effects on acute episodes of a wide range of tissues. Ibuprofen was the first phenylpropionate to be marketed in the United States. It has analgesic, antipyretic and anti-inflammatory activity and it is well absorbed and well tolerated (134, 135). Ibuprofen has also been shown to improve several aspects of the wound healing ranging from wound edema. As previously described in literature the second degree burn wounds treated with Ibuprofen 5 % from two and five hours after burn showed a significantly reduced lymph drainage and no variation in the wound water content (136).

1.6 Main goals of the present study

In this study new skin substitutes were aimed to be produced. The objectives of the workplan comprised:

1) Production of Chitosan-Gelatin sponge using freeze-dried method;
2) Coating of sponges with nanofibers produced with Chitosan deacetylation, PEO, PCL and Ibuprofen);
3) Morphological and physicochemical characterization of the bilayer of the S;
4) Evaluation of biocompatibility of the developed system;
5) Evaluation of the antibacterial properties of the produced S.

Chapter II- Materials and Methods

2. Materials and Methods

2.1 Materials

The cell culture plates and T-flasks used in this study were obtained from Orange Scientific (Brainel' Alleud, Belgium). Cell imaging plates were purchased from Ibidi GmbH (Munich, Germany). Lysozyme (46 400 U/mg) and 3-(4,5-Dimethyl-2-thiazolyl)-2,5-diphenyl-2H-tetrazolium bromide (MTT) were purchased from Alfa Aesar (Karlsruhe, Germany). Ibuprofen was purchased from TCI (Tokyo Chemical Industry, Co., LTD., Japan). Chitosan (medium molecular weight (MMW) 190,000-310,000 $g.mol^{-1}$) and (low molecular weight (LMW) 50.000-190.000 $g.mol^{-1}$), Dulbecco's Modified Eagle's Medium (DMEM-F12), Gelatin, glutaraldehyde, kanamycin, sodium hydroxide (NaOH), streptomycin, tripolyphosphate (TPP), trypsin, PEO and PCL, amphotericin B, Ethanol (EtOH), paraformaldehyde (PFA) and trypan blue were purchased from Sigma-Aldrich (Sintra, Portugal). Acetic acid was acquired to Pronalab (Barcelona, Spain). Normal human dermal fibroblasts (NHDF) criopreserved cells were purchased from PromoCell (Labclinics, S.A.; Barcelona, Spain). *Staphylococcus aureus* was isolated in the clinic. Fetal bovine serum (FBS) was purchased from Biochrom AG (Berlin, Germany). LB Broth was obtained from Liofilchem (Via Scozia, Italy). Propidium Iodide (PI) was purchased from Invitrogen (Carlsbad, USA).

2.2 Methods

2.2.1 Sponge production

S were produced through freeze-drying, as preiously described elsewhere (137). First, MMW Chitosan 2 % (w/v) was dissolved in a solution of 1 % (v/v) acetic acid and 4 % (w/v) Gelatin was solubilized a Mili-Q water. The samples were stirred for 24 hours at 50 ºC to obtain a homogenized solution. Following this, the solution was placed in cylindrical mold and taken to -80 ºC, for 14 hours and then lyophilized (Scanvac CoolSafe™, ScanLaf A/S, Denmark) for 24 hours. The lyophilized structures were recovered from the molds and crosslinked with TPP 2 % (w/v) for 4 hours at room temperature (RT). After that, the cycle of freezing and freeze-drying was repeated.

2.2.2 Production of membrane and coated sponge

2.2.2.1 Deacetylation of Chitosan

The LMW Chitosan was deacetylated and further purified in order to improve the surface charges to increase its possible the interaction with cells (113). Subsequently, Chitosan was dissolved in a NaOH solution. 500 mg of Chitosan was mixed with 10 mL of NaOH (1 M). After that, the mixture was heated at 50°C, under magnetic stirring for 4 hours and then filtered

through a 0.44 µm filter in a Buchner funnel. The remaining material was washed extensively until the pH was equal to that of ultrapure water. Finally, the samples were dried at 40°C overnight (138).
In order to determine the DD, the recovered deacetylated Chitosan was dissolved in acetic acid (1 M). The solution was then filtered with a 0.22 µm filter to remove any solid particles. Subsequently, the pH was adjusted to 7 with NaOH (1 M). The product was then centrifuged three times at 4500 rpm (Sigma 3K18C centrifuge) and finally the recovered pellet was freeze-dried for 24 hours. The DD was measured by determining the first derivative of UV-vis spectrum (139).

2.2.2.2 Electrospinning setup

The system used to produce the M and CS was composed by a high power voltage supply (Spellman CZE1000R, 0–30 kV), a syringe pump (KDS-100), a syringe fitted with a stainless steel blunt end needle and an aluminum plate connected to a conductive collector. The needle was positively charged by the power supply and the metal collector was grounded. The charged tip and grounded collector form a static electric field between them, to provide the driving force that enables fiber formation (91, 140).

2.2.2.3 Production of Chitosan/PEO/PCL/Ibuprofen electrospun membrane

Two solutions were prepared separately: (i) 1.2 g of deacetylated Chitosan (obtained as previously described in section 2.2.2.1) was dissolved in 90 % acetic acid and 0.25 g of PEO; and (ii) 1 g of PCL and 0.16 mg/mL of Ibuprofen was dissolved in pure acetone. Then these to solutions (Chitosan/PEO and PCL/Ibuprofen) were mixed at a ratio of 1:1 (v/v) under stirring until a homogenized solution was obtained. Then Ibuprofen at a final concentration of 0.8 mg/ml was added to the mixture.
The previously prepared solutions were placed in a 10 ml plastic syringe. The solution flow rate was set to 1-2 ml/hour. The electric voltage applied was 20-25 kV and the ground collector was at 10 cm from tip of the syringe needle. All experiments were conducted at ambient pressure and relative humidity of 15-20 % (141).

2.2.3 Characterization of the physicochemicals properties of sponge, membrane and coated sponge

2.2.3.1 Scanning electron microscopic analysis

The morphologies of S, M and CS were characterized by SEM. The samples were frozen using liquid nitrogen and freeze-dried for 3 hours. Subsequently, they were mounted on aluminum stumps, coated with gold using a Quorum Q150R ES sputter coater. Then, samples were

analyzed using a Hitachi S-3400N scanning electron microscope operated at an accelerating voltage of 20 kV and at different magnifications.

2.2.3.2 Fourier transform infrared spectroscopic spectroscopy analysis

FTIR analysis is extensively applied for identify the chemical structure of samples (S, M and CS) by comparing their spectra with the spectra of the materials used for their production (Quitosan LMW and MMW, Gelatin, TPP, PEO, PCL and Ibuprofen). In this technique, the radiation crosses the sample and some of it is absorbed, while other part is transmitted. The resulting spectra represent the frequency of vibration between the atoms linkage from the sample, creating therefore, a specific spectra for those interactions (142). The FTIR spectra of the samples were acquired with a spectrophotometer Nicoletis 20 (64 scans, at a range of 4000 to 1000cm^{-1}) from Thermo Scientific (Waltham, MA, USA) equipped with a Smart Itr auxiliary.

2.2.3.3 Contact angle determination

Contact angles of the surface of S, M and CS were determined using a data physics contact angle system OCAH 200 apparatus, operating in static mode. For each sample, water drops were placed at various locations of the materials surface at RT. The reported contact angles are the average of at least three measurements (143).

2.2.3.4 Swelling studies

The water uptake capacity of the samples (S, M, CS) were determined using a sample gravimetric method (144). Samples were weighted and incubated in falcons with 5 mL of solution phosphate buffered saline solution (PBS) at 37 ºC, and at pH 5.5 and pH 7.4. At predetermined intervals, the samples were recovered from PBS solution and weighed. Then they were re-immersed into the swelling medium. After, the swelling ratio percentages were determined using the following equation:

$$\text{Swelling ratio } (\%) = \frac{\text{weight} - \text{initial weight}}{\text{initial weight}} \times 100 \quad (1)$$

2.2.3.5 Porosity evaluation

The total porosity of the samples (S, M and CS) was determined by adapting a displacement method (145). The total amount of ethanol (100 %) that the samples were able to absorb in 4 hours, was used to determine the porosity of the samples using the following equation:

$$\text{Porosity } (\%) = \frac{\text{weight swollen sponge} - \text{initial weight}}{\text{density etanol} - \text{volume sponge}} \times 100 \quad (2)$$

2.2.4 Characterization of sponges and coated sponges through *in vitro* assays

2.2.4.1 *In vitro* degradation assays

S and CS samples (n=3) were incubated in 10 mL of PBS with or without lysozyme (10 mg/L). Samples were maintained at 37 ºC for 21 days (144). After 1, 4, 7, 14 and 21 days samples were removed, rinsed twice with distilled water and dried on the lyophilizer. After, samples were weighted in order to determine the percentage of weight loss, through equation:

$$\text{Weight loss } (\%) = \frac{\text{inicial weight} - \text{final weight}}{\text{initial weight}} \times 100 \qquad (3)$$

For complementar analysis, SEM images were also acquired to characterize the morphology and porosity of the samples for each degradation period.

2.2.4.2 Proliferation analysis of NHDF cells in contact with samples

NHDF cells were seeded in T-flasks of 25 cm^2 with 6 mL of DMEM-F12 supplemented with heat-inactivated 10 % FBS (v/v) and 1% antibiotic/antimycotic solution. Hereafter, cells were kept in culture at 37 °C in a 5 % dioxide carbon (CO_2) humidified atmosphere, inside an incubator (146). When cell confluence was achieved, cells were sub cultivated by 3-5 minutes incubation in 0.18 % trypsin (1:250) and 5 mM ethylenediaminetetraacetic acid (EDTA). Then, cells were centrifuged, resuspended in culture medium and then seeded in T-flasks of 75 cm^2 and maintained in culture using the same conditions.

To evaluate cell viability in the presence of the samples (S, M and CS) herein produced, each sample were added (n=5) into a 96-well cell culture plates. Previously to cell seeding samples were sterilized by UV exposure for at least 30 min.

NHDF cells were seeded at a density of $2x10^4$ cells per well in 96-well plates containing the samples (S, M and CS). Cells where maintained in DMEM-F12 supplemented with heat-inactivated 10 % FBS (v/v). Hereafter, cells were kept in culture at 37 °C, in a 5 % CO_2 humidified atmosphere, inside an incubator (146). After 24, 48 and 72 hours of cells being in contact with samples (S, M and CS) were monitored by Olympus CX41 inverted light microscope (Tokyo, Japan) equipped with an Olympus SP-500 UZ digital camera (143, 146) was used to monitor cellular growth.

The biocompatibility of the samples was also evaluated, after cells being in contact with the samples during for 24, 48 and 72 hours, through an MTT assay was performed. Briefly, the culture medium of each well was removed and replaced with a mixture of 100 µL of fresh medium and 20 µL of MTT reagent solution. After a period of 4 hours of MTT incubation at 37 °C, under a 5 % CO_2 humidified atmosphere, the medium was aspirate leaving just the formazan crystals. These crystals were dissolved with 200 µL Dimethylsulfoxide (DMSO) using on orbital

shaker. After, the absorbance of the produced formazan was measured at 570 nm using a microplate reader (BIO-RAD xMark ™ Microplate Spectrophotometer) (147). Wells containing cells in the culture medium without any sample were used as negative control. 70% EtOH was added to other wells containing cells which and were used as positive control (66).

2.2.4.3 Scanning electron microscopic analysis of cells adhesion

Cells adhesion of the S, M and CS were analysed by SEM. After 24, 48 and 72 hours of culture, samples with cells were recovered and washed in PBS. Then, samples were emerged in 2.5 % (v/v) glutaraldehyde at 4ºC to fix cells (144). Samples were then frozen using liquid nitrogen and freeze-dried for 3 hours. Subsequently, samples were mounted on aluminum stumps, coated with gold using an Quorum Q150R ES sputter coater (137). Lastly, samples were analyzed using a Hitachi S-3400N scanning electron microscope operated at an accelerating voltage of 20 kV and at different magnifications.

2.2.4.4 Confocal microscopic analysis of the sponge and coated sponge

CLSM was used to evaluate the ability of cells to become internalize in the samples. For the visualization of NHDF cells within samples (S and CS), 1×10^4 cells/well were seeded in µ-Slide 8 well Ibidi imaging plates (Ibidi GmbH, Germany) in contact with samples. After 24 hours, cells were fixed with 4 % PFA for 20 min. After, cells were stained with 1 µL of PI (1 mg/mL) during 15 min, at 37 ºC. Then, the PI solution was washed and the samples were washed three times with PBS. Imaging experiments were performed in a Zeiss LSM 710 CLSM (Carl Zeiss SMT Inc., USA), where consecutive z-stacks were acquired. 3D reconstruction and image analysis was performed in Zeiss Zen 2010 (143).

2.2.5. Incorporation of Ibuprofen in sponges

2.2.5.1 IC50 determination of the Ibuprofen in NHDF cells

To determine IC50 of Ibuprofen for NHDF cells, cells were initially seeded at a density of $2x10^4$ cells/well in a 96-well cell culure plates, containing DMEM-F12 supplemented with 10 % FBS (v/v). Adherent cells were grown at 37 °C, in an incubator with a humidified atmosphere containing 5 % CO_2. In the following day, culture medium was replaced and cells were incubated with crescent concentrations of Ibuprofen (0.25, 0.50, 0.70, 0.75, 0.80 and 0.90 mg/mL). Wells containing cells in the culture medium without Ibuprofen were used as negative control. EtOH 70 % was added to wells containing cells that were used as positive control.

2.2.5.2 Characterization of the Ibuprofen release profile

The release studies were performed in order to evaluate the rate of drug release from the samples. First, 10 mL of PBS was added to a falcon, at 37º C, pH=7.4. Afterwards, 1 mL of the samples were periodically taken along 50 hours and substituted by equal amount of PBS. Spectra of the recovered samples were acquired using a UV-1700 PharmaSpec spectrophotometer from Shimadzu (Kyoto, Japan) and analyzed with an UVProbe Shimadzu 2.0 software. The absorbance of various samples concentrations of Ibuprofen in PBS was determined at 264 nm. A drug calibration curve was performed usind various concentrations of Ibuprofen (0.05, 0.1, 0.2, 0.4, 0.5 mg/mL), and determining their absorvance at 264 nm.

2.2.5.3 Characterization of the cytotoxic profile of the samples loaded with Ibuprofen

The Ibuprofen cytotoxic profile was characterized by means of *in vitro* assays. The MTT assay (described in detail in topic 2.2.4.2) was performed to further evaluate the cytotoxicity of this drug. The absorbance of the produced formazan was measured at 570 nm using a microplate reader (BIO-RAD xMark ™ Microplate Spectrophotometer) (147). Wells containing cells in the culture medium without any sample were used as negative control. 70 % EtOH was added to wells containing cells, that were used as positive control.

2.2.6 Sponge and coated sponge antimicrobial activity

To evaluate the antimicrobial effect of the S and CS, *Staphyloccocus aureus* was used as a model of Gram-positive bacteria usually present in skin injuries. The bacterial culture medium (LB Broth) was inoculated with *Staphyloccocus aureus* at a concentration of $1x10^8$ colony-forming units (CFU)/ml. A negative control was prepared without samples and a positive control was prepared with addition of the Kanamycin antibiotic (2µL). Then, 2 ml of inoculum were added to an agar petri dish using scattering method. Samples (S and CS) were previously sterilized with UV for 30 minutes, and then placed on the plates. The plate was incubated 24 hours at 37 ºC. After incubation, the halos that resulted from the inhibitory effect of S and CS were observed macroscopicaly. After the bacterial assay, materials were removed from the agar plate and fixed in glutaraldehyde overnight. They were subsequently frozen in liquid nitrogen (-180 °C), lyophilized and analysed by SEM. The inhibitory halo was measured using an image analysis software—ImageJ (148) .

2.2.7 Statistical analysis of the results

Statistical analysis of the obteined results were performed, using one-way ANOVA with the Dunnet's post hoc test and Newman- Keuls multiple comparison test. Each result is the mean ± standard error of the mean of at least three independent experiments (82)

Chapter III -Results and Discussion

3. Results and Discussion

3.1 Characterization of the properties of sponge, membrane and coated sponge

The Chitosan is known by its antitumoral, antifungal and antimicrobial activity (149). Furthermore, Chitosan and its derivatives are also known by their capacity to improve the wound healing process by enhancing the functions of inflammatory cells such as macrophages. Chitosan can also increase the tensile strength of wounds (150).

For skin regeneration, the antimicrobial activity of Chitosan against different microorganisms is very important. There are two main mechanisms associated with inhibition of microbial cells by Chitosan (151). The interaction of Chitosan with the anionic groups on the cell surface that causes the formation of an impermeable layer around the cell that prevents the transport of essential solutes.

Chitosan degree of deacetylation (DD) and Molecular weight (MW), have also influence on its antimicrobial activity, hydrophilicity, degradation and cell response (152). The number of free amino groups increases with the DD and these groups are able to interact with the membrane. It was reported that Chitosan with relatively high DD 89 % strongly stimulated fibroblast proliferation, while samples with lower DD showed a lower cellular growth.

Taking these facts into account it is fundamental that 3D constructs be built with Chitosan with LMW and a high DD. In this work LMW Chitosan was further deacetylated. The DD of the commercial LMW Chitosan is defined as the percentage of primary amine groups in the Chitosan structure. Chitosan DD can be controlled by processing the polymer with an alkaline treatment (e.g. NaOH) (153). This allows the interaction between Chitosan and cells, stimulating their adhesion and proliferation and also improving its antimicrobial and haemostatic activities, thus enhancing Tissue Regeneration (71, 122). The results obtained herein demonstrate that the percentage of DD Chitosan obtained was around 96 % (Table 2), which is higher than that of the commercial one (153).

Table 2: DD of the commercial LMW Chitosan and of the deacetilated Chitosan produced herein (mean ± SD, n=3). The nominal DD was provided by the manufacturer. The DDs were determined by the first derivation of the UV-VIS spectrum of Chitosan.

Sample	Nominal DD (%)	Determined DD (%)
Comercial LMW Chitosan	75-85	90.02 ± 1.87
Deacetilated Chitosan	-	95.88 ± 1.19

3.2 Morphologic characterization of the samples

3.2.1 Membrane morphology

The M consisting of Chitosan, PEO and PCL was produced by electrospinning. Macroscopically it is possible to observe that the M is formed by a homogenous and dense structure of fibers (Figure 16 A1). A more detailed analysis through SEM image of the M reveals its dense 3D nanofiber network comprised by randomly arranged fibers, which results in an interconnected porous structure (Figure 16 A2). This 3D organization creates a large contact area with anchoring points for cell-nanofiber interactions enhancing cell adhesion, migration and proliferation (154). The porous nature is beneficial for cellular infiltration and proliferation (155). Additionally, porosity also ensures a correct gas, nutrient and fluids exchanges, processes that are fundamental for obtaining hemostasis and proper wound healing (155).

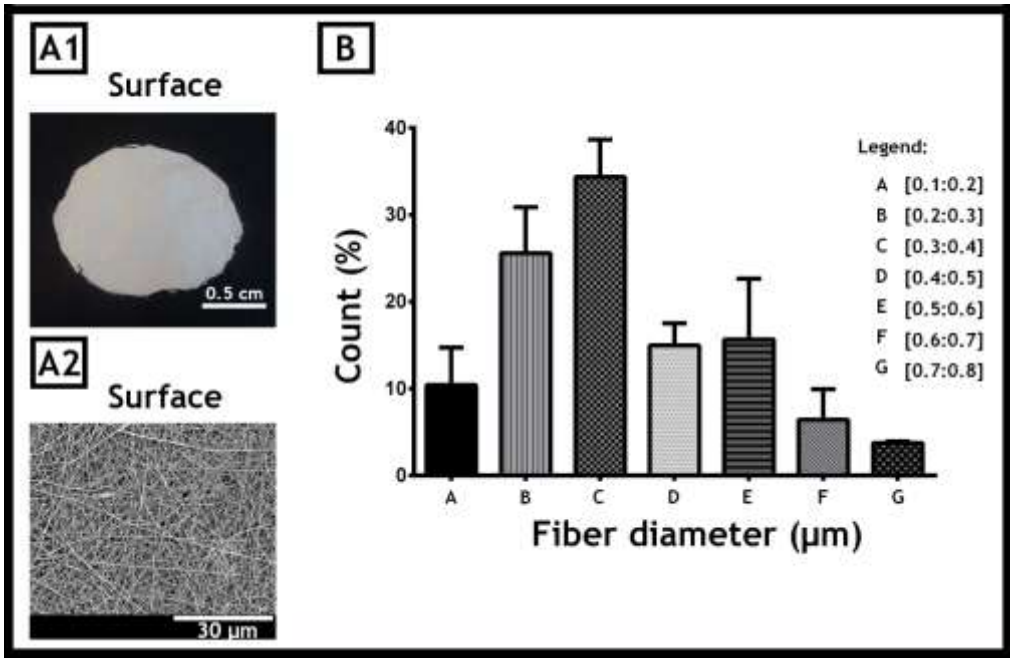

Figure 16: Macroscopic (A1) and SEM images (A2) of the M. Graphical representation of fiber diameter ranges (B) from 142 measures by using Image J.

The distribution of the fibers diameter was measured using the image processing program Image J (148). The most common fiber diameter was around 0.3 and 0.4 μm (Figure 16 B). Although it is important to achieve M mostly constituted by nanofibers with few hundred nanomaters of diameter, once it is described that the reduction of the diameter of the fibers leads to an increased cell adhesion and proliferation (156). The fiber diameter is also an importante feature that influence the release of bioactive molecules (93) through diffusion (93).

3.2.2 Sponges and coated sponges morphology

The sponges produced in this work were obtained by a freeze-drying method, where the formation of ice crystals improved the porosity of the samples (Liapis et al., 1996). In Figure 17 it is possible to observe that the design S and CS have a porous and interconnected 3D structure. In SEM images, demonstrate that the CS is perfectly covered by the nanofibers (Figure 17 B c), and d)). The S and CS possess continuous interconnected pores up to 400-500 μm of diameter. Pore size is an important condition for skin regeneration. If pores are too small, cells will cover the pores, influencing cell migration and inhibiting neovascularization. On the other hand, if they are too large a decrease in cellular adhesion can occur.

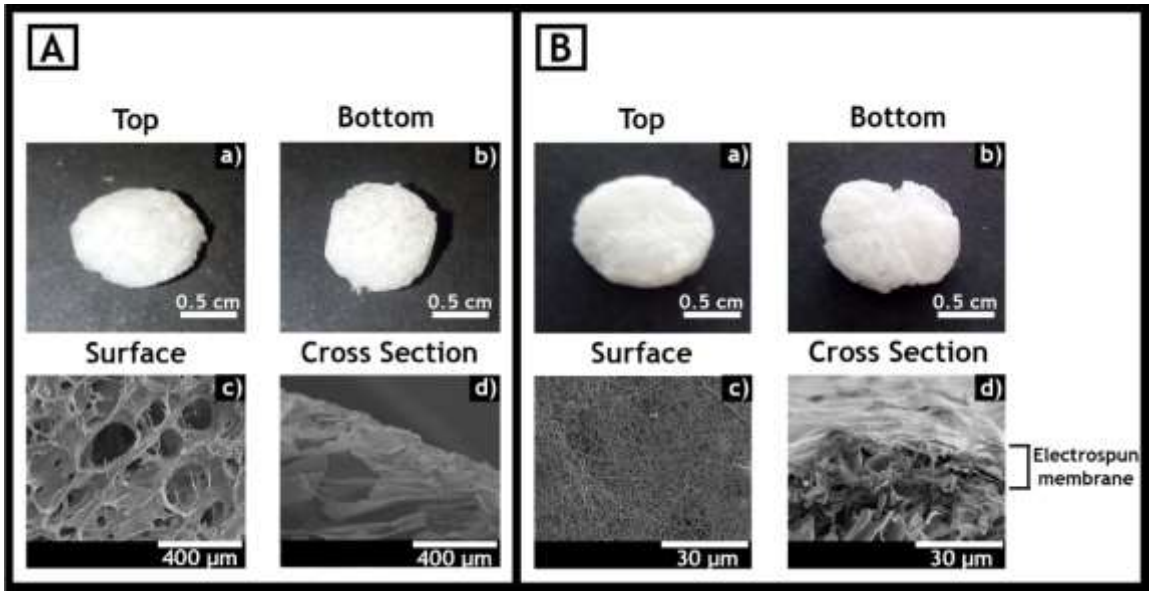

Figure 17: (A) Macroscopic and microscopic images of S. (B) Macroscopic images and microscopic images of CS.

For better characterize the porosity of the samples, liquid displacement method using ethanol was also performed (Figure 18).

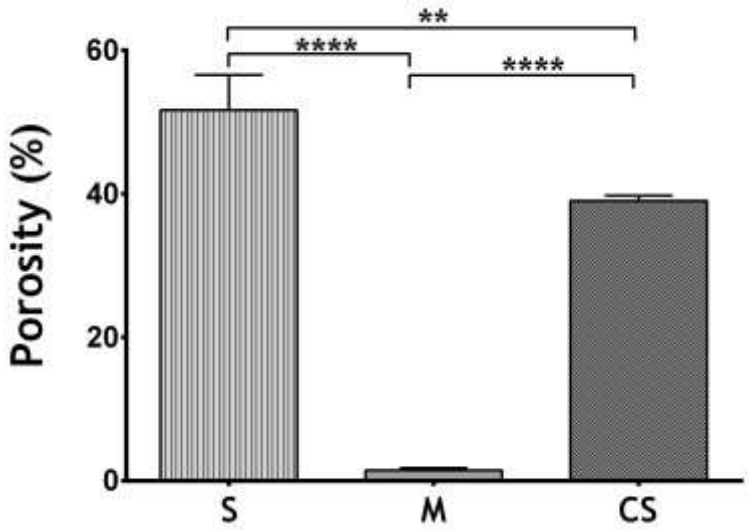

Figure 18: Determination of the porosity of S, M and CS. Where ** represents p<0.001 and **** p<0.0001.

Accordingly to SEM images, S presented the highest value of porosity 51.60 % ± 2.45, when compared with the CS 39.00 % ± 0.37 and M 1.50 % ± 0.17. However even CS has a good percentage porosity for cell migration, adhesion, proliferation and also the diffusion of nutrients, oxygen and waste products, leading to an improved wound healing (143).
The Chitosan/Gelatin sponges obtained by the freeze-drying method are highly porous, allowing the unhindered diffusion of solutes and nutrients. Also, the interconnectivity between the pores provides more space and surface area-to-volume ratio for cell growth and local angiogenesis (146). Pores also promote fluids drainage, which is fundamental to prevent the build-up of exudates (66).

3.3 Fourier transform infrared spectroscopic analysis of the sponge, membrane and coated sponge

In infrared spectroscopy the radiation crosses the sample and some of it is absorbed, while other part is transmitted. The resulting spectra represent the frequency of vibration between the atoms linkage from the sample, creating therefore, a specific spectra for those interactions (142). The FTIR analysis of the freeze-dryed sponges was performed to characterize the chemical composition of the different samples (Figure 19).

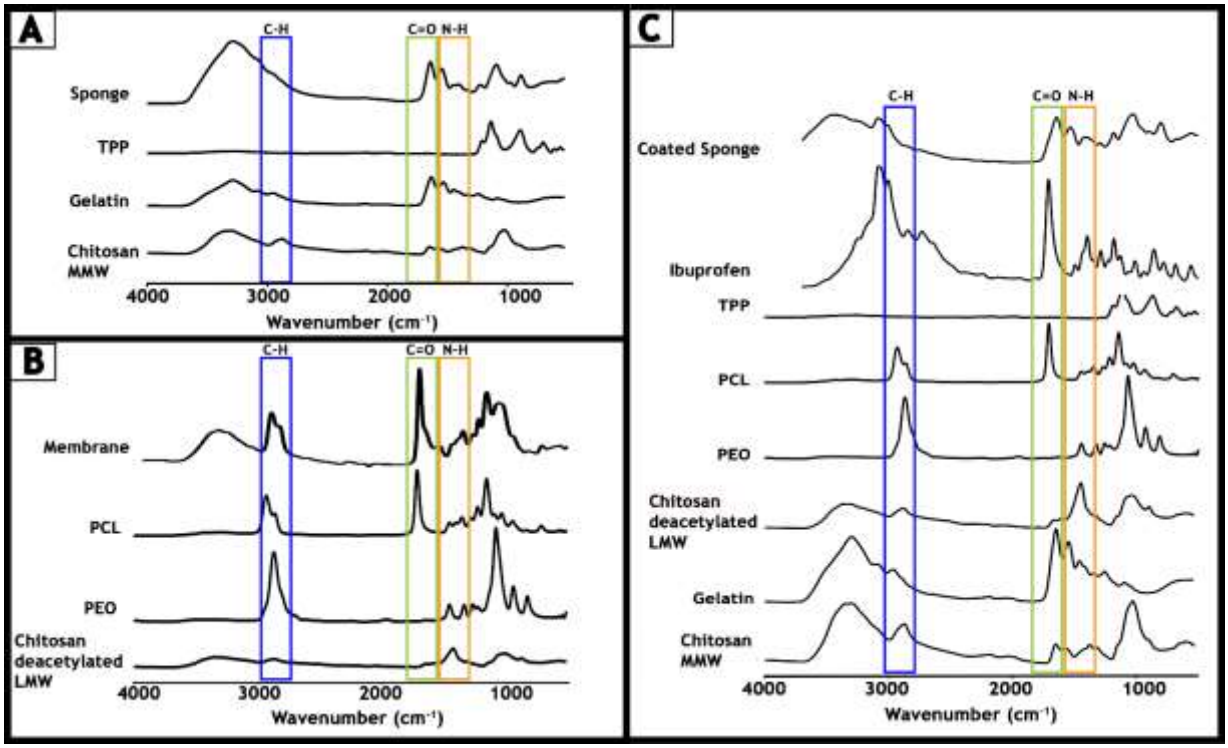

Figure 19: FTIR spectra of the produced S (A), M (B) and CS (C) and respective constituents: Quitosan MMW, Quitosan deacetylated LMW, Gelatin, TPP (Tripolyphosphate), poly (ethylene oxide (PEO)), poly (ε-caprolactone) (PCL) and Ibuprofen.

The characteristic peaks of TPP, Gelatin and MMW Chitosan are observed in the S (Figure 19 A). In previous studies it was reported that the MMW Chitosan present characteristics peak at 1640 cm^{-1} (C=O stretch in primary amide) and 1546 cm^{-1} (N-H stretch in primary amine) (157). The other characteristic peak is observed at 3266 cm^{-1}, that confirms the presence of Chitosan owing to the N-H group stretching in the polysaccharide, as referred by Bhat and collaborators (158). Gelatin present bands at 3284 cm^{-1} (N-H in amines), 1633 cm^{-1} (C=O stretch in primary amide) and 1531 cm^{-1} (N-H deformation in secondary amides).

The spectrum of the LMW deacetylated Chitosan (Figure 19 B) shows a variation in the wavelength of the peak from 1546 to 1433 cm^{-1}, indicating that the secondary amide (—NH—R) has been further changed to primary amide (—NH2) by alkaline deacetylation (157). The process of deacetylation of Chitosan was achieved, leading to and increase in the number of amine groups at its surface. The electrostatic interaction between the positive charges of the amine groups of Chitosan and negative charges of phospholipids of cell membrane is more efficient.

The nanofiber present in M (Figure 19 B), show characteristic PCL peak at 1723 cm^{-1}, and the C-H stretching region of FTIR spectrum, the higher intensity peak at 2936 cm^{-1}. PEO presents the characteristics peaks at 2875 cm^{-1} in the C-H stretching.

In relation to CS, all its characteristic peaks are present in the spectrum (Figure 19 C). Also, it is possible to observe the representative peaks of the Ibuprofen, being the most characteristic the ones present at 2870 and 2727 cm^{-1} highlighted by the C-H stretching vibrations peaks that

correspond to the alkyl groups of Ibuprofen. The sharp peak at 1702 cm^{-1} belongs to a carboxyl vibration, that is characteristic of Ibuprofen (159).

3.4 Contact angle of the sponge, membrane and coated sponge

The determination of contact angle is important to verify the hydrophobicity of the samples, since it interferes with cellular behaviour and then influence the tissue regeneration. It is known that hydrophilicity improves Tissue Regeneration by allowing cell migration, adhesion, proliferation and also the diffusion of nutrients (143).

The contact angle is defined as the angle formed by the intersection of the liquid-solid interface and the liquid-vapor interface (geometrically acquired by applying a tangent line from the contact point along the liquid-vapor interface in the droplet profile). Small contact angles 90° correspond to high wettability, while large contact angles correspond to low wettability i.e. hydrophobic character. Since PCL is a hydrophobic compound, its application will confer a hydrophobic character to M, that showed, contact angle 96.24º ± 4.70. The S and CS are both hydrophilic, having contact angles of 71.14 º ± 2.55 and 45.64 º ± 6.08, respectively (Table 3).

Table 3: Contact angles determined for the produced samples.

Materials	Water contact angle
S	71.14º ± 2.55 º
M	96.24º ± 4.70º
CS	45.64º ± 6.08º

The sponge coating confers a more hydrophilic character to CS and improved cell adhesion and proliferation, wich are fundamental for skin regeneration.

3.6 Characterization of swelling profile of the sponge, membrane and coated sponge

Polimeric biomaterials tend to absorb fluids due to osmotic pressure in order to fill the void regions of the polymeric network and within the beads that remained dehydrated, until they reach the equilibrium state. The water uptake causes an increase in the pore diameters allowing a subsequent diffusion of cells, nutrients, bioactive molecules and waste products through the biomaterials, which is for essential in skin regeneration. Also, the swelling profile of the samples are fundamental for the wound cleaning and allowing exudates removal.

The swelling studies are important to notice that the solvent used for the assay must have similar properties to that the fluids present in skin wounds. Therefore, the swelling test was conducted by immersing materials in PBS at pH 7.4 and 5.5.

The swelling degree is dependent on the pore size of samples and on the polymer-solvent interactions (160-162). S and CS have a very porous structure, as a consequence, these sponges had higher percentages of sweeling ratio, between 800-1000 % in both the CS (Figure 22) and in S (Figure 20). It is noteworthy that at pH 7.4 the swelling was always higher whereof pH 5.5. Such swelling behaviour can be explained by the presence of hydrophilic groups in Chitosan and Gelatin, such as hydroxyl, amino and carboxyl groups that can be easily hydrated (31, 163).

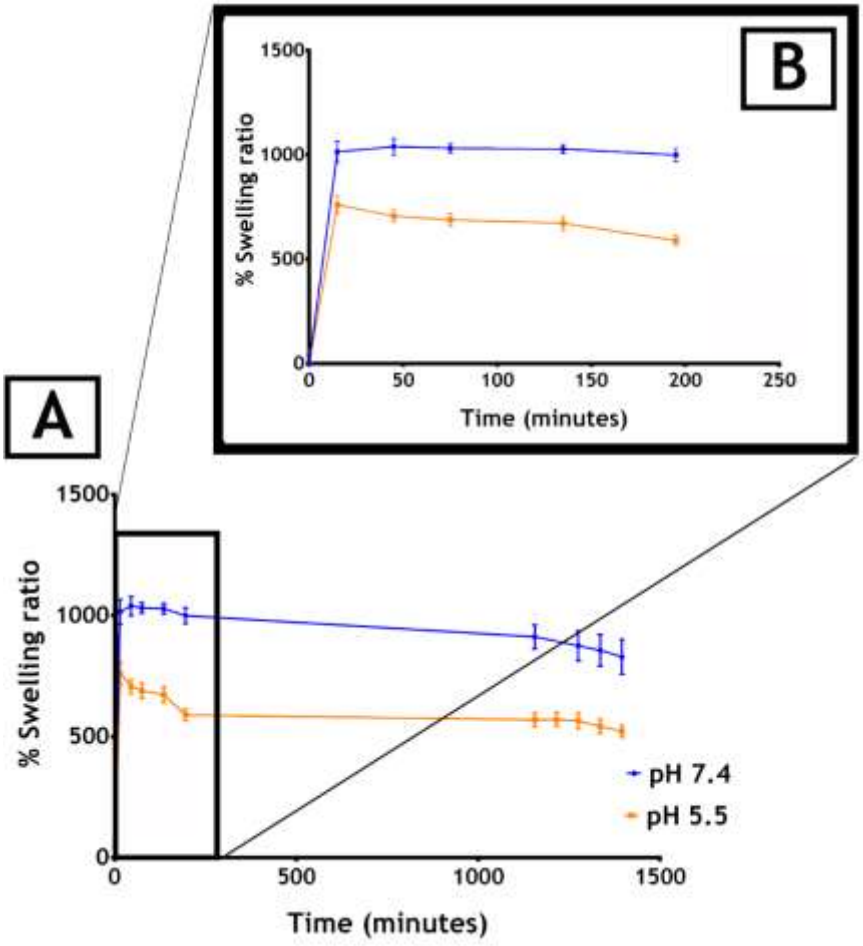

Figure 20: Swelling profile of the produced S (A) and close-up of the first 250 minutes (B). The swelling studies were carried out at pH 7.4 (shown in blue) and pH 5.5 (shown in orange).

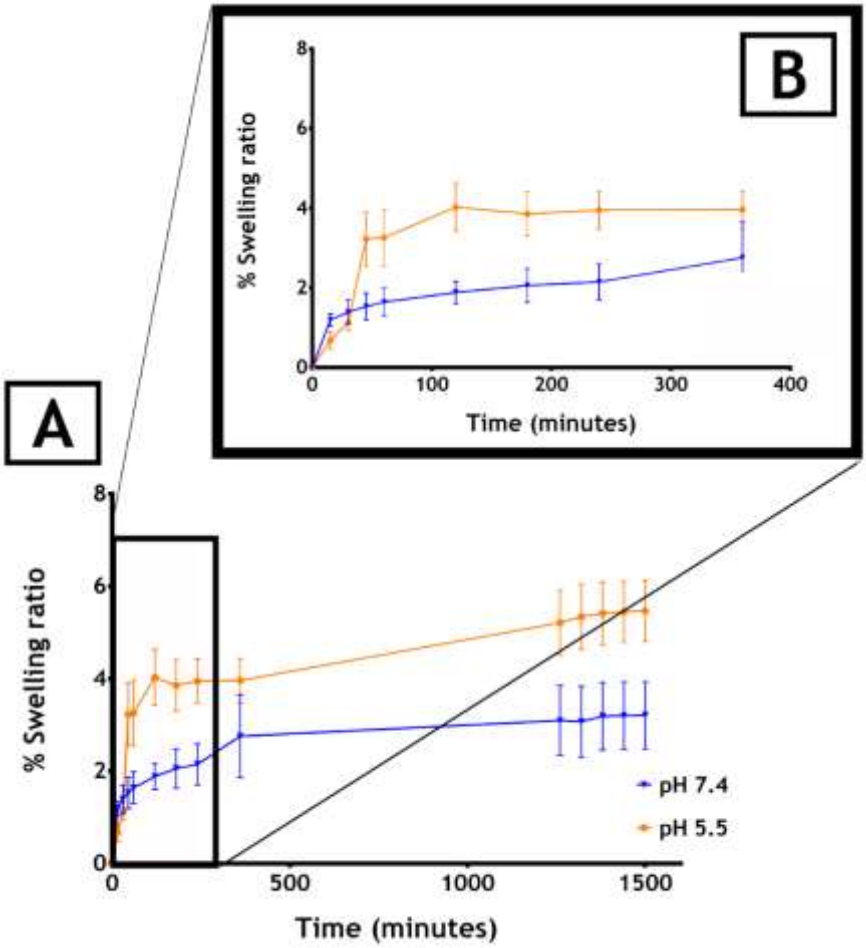

Figure 21: Swelling profile of the produced M (A) and a close-up of the first 400 minutes (B). The swelling studies were carried out at pH 7.4 (shown in blue) and pH 5.5 (shown in orange).

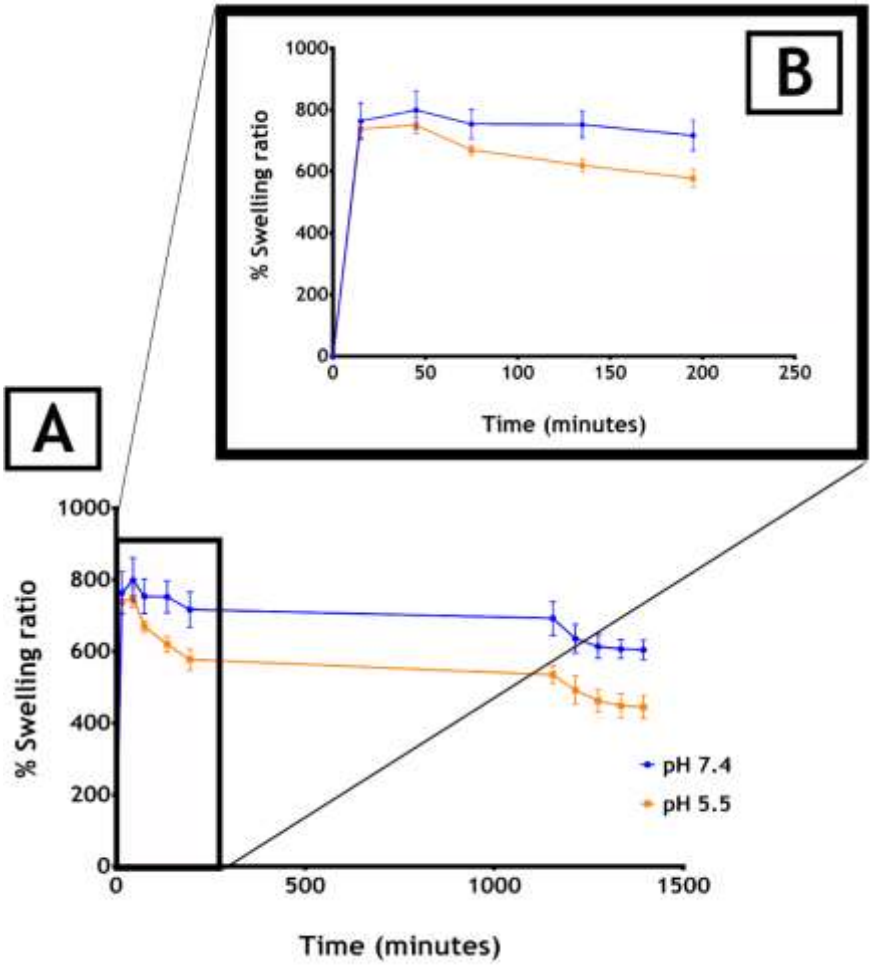

Figure 22: Swelling profile of the produced CS (A) and a close-up of the first 250 minutes (B). The swelling studies were carried out at pH 7.4 (shown in blue) and pH 5.5 (shown in orange).

The M swelling profile percentage is very low (Figure 21) in accordance with its hydrophobic constituition (PCL) and low degree of porosity. Such may be responsible for the lower swelling ratio percentage of CS in relation to S. The swelling percentage of CS is approximately 800 % (86, 164). Such result may be explained through the lower porosity of CS, since it is coated with PCL.

3.7 *In vitro* degradation of the sponge and coated sponge

While occurs the formation of a new tissue it is also important to ensure that materials are degradaded in order to allow cell growth.

To study the degradability of the biomaterials produced, their degradation studies. In these profile was studied *in vitro*, sponges were immersed in a saline solution with enzymes that are involved in the degradation of the biomaterials that constitute the 3D construct. The determination of weight loss allow to characterize materials degradation profile. The degradation study was performed with PBS and PBS plus Lysozyme (enzyme present in human

body that is responsible for Chitosan degradation). In Figure 23 A and 24 A are represented the degradation over time of the S and CS in solution of PBS and PBS plus Lysozyme.

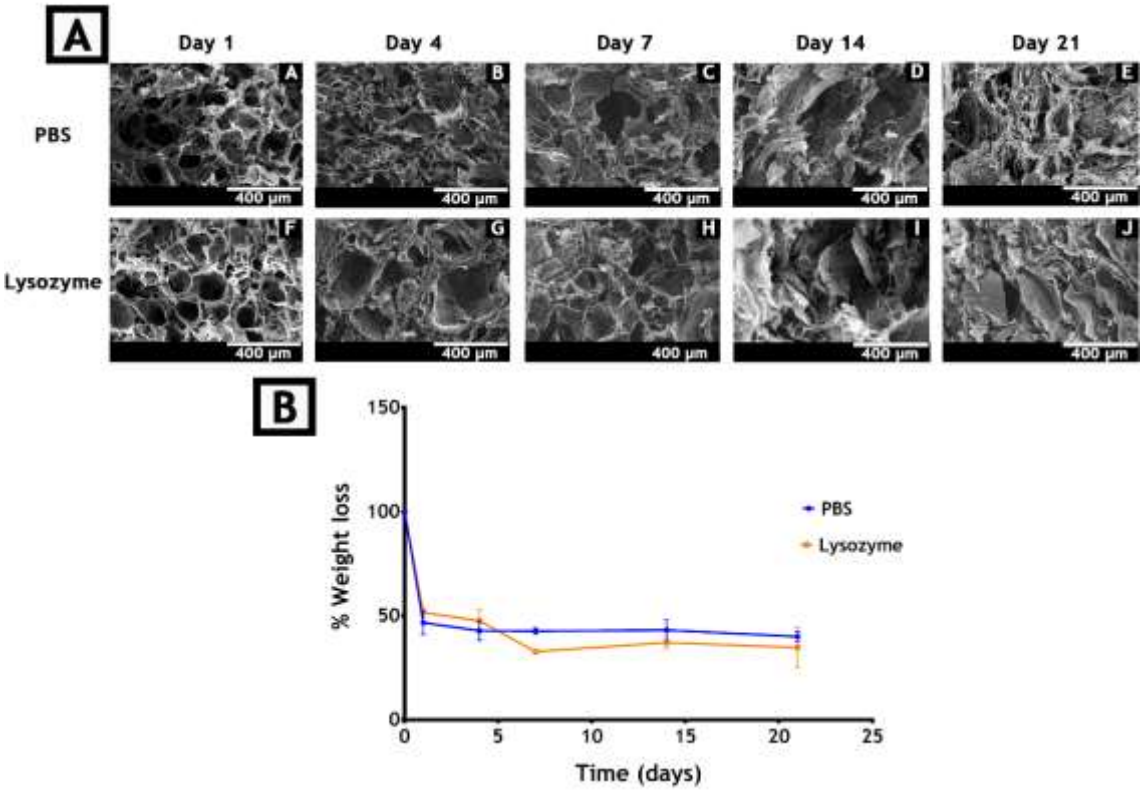

Figure 23: Charactherization of the degradation profile of S. SEM images (A) and weight loss along time (B). The tests were performed during 1, 4, 7, 14 and 21 days, in PBS and PBS plus Lysozyme. The pH of the solutions was set to 7.4.

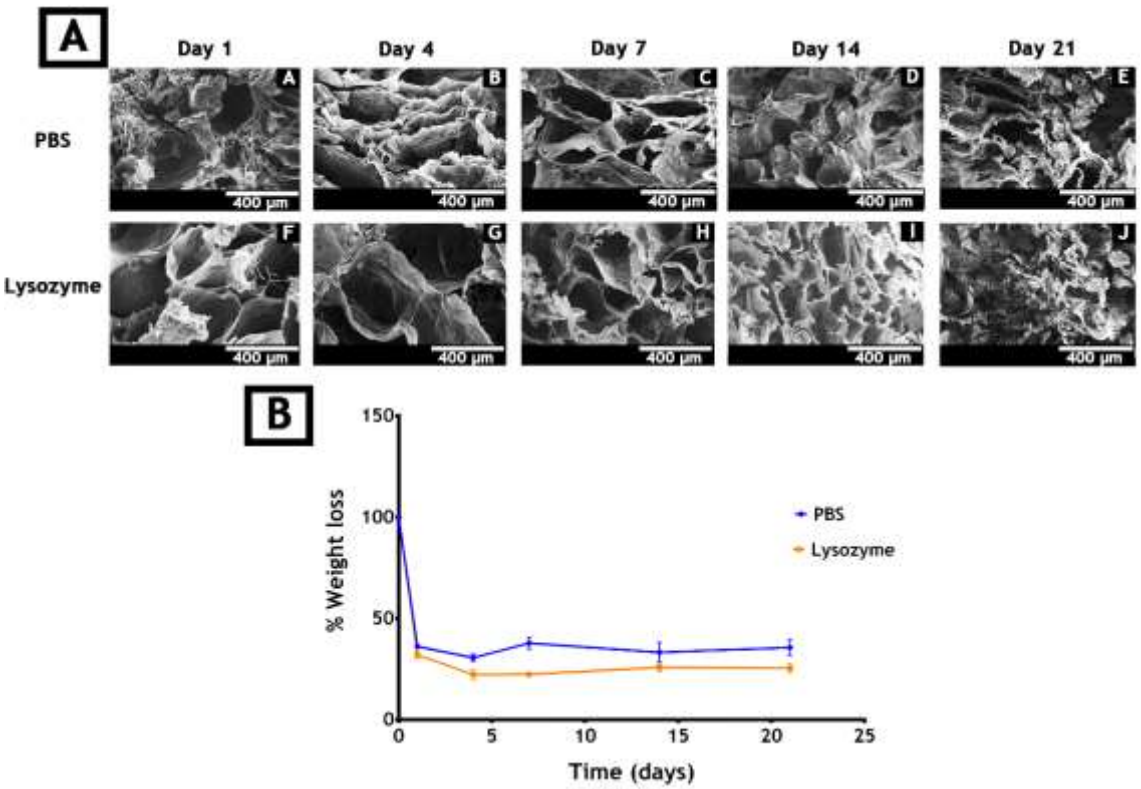

Figure 24: Characterization of the degradation profile of CS. SEM images (A), and graph representation (B). The tests were performed during 1, 4, 7, 14 and 21 days in solutions of PBS and PBS plus Lysozyme. The pH was set to 7.4.

In Figure 23 B and 24 B, it was noticed that after 24 hours both samples (S and CS) had a weight loss of about 50 % in PBS and Lysozyme. Nevertheless, as expected in the presence of Lysozyme the degradation degree was higher (Figure 23 B and 24 B). In conclusion, it can be concluded that sponges, suffer a high degree of degradation when immersed in the lysozyme solution.

3.8 Evaluation of cellular viability and cell proliferation in contact with sponge, membrane and coated sponge

As already previous described above it is very important to produce biocompatible materials. The biocompatibility of a biomaterial is important since it should be capable of elicit an appropriate response for a specific application, and also do not trigger on, inflammatory or toxic reaction when in contact with a live tissue or body fluids. The cellular viability of NHDF in contact with the produced sponges was quantitatively measured at 24, 48 and 72 hours using an MTT assay. The values of absorbances obtained for formazan are directly proportional the number of viable cells.

Fibroblasts cells were chosen, due to their potential for skin regeneration, since they synthetized ECM proteins (e.g. collagen and fibronectin), cytokines (IL-6 and TNF-α) and growths factors that are essential for the wound healing process (42).

The results of the MTT assay (Figure 25) show that the produced sponges are biocompatible, displaying a higher cell viability than the positive control (k+), however lower than negative control (k-). The cellular viability is higher than 70 % wich is in accordance with the during requirements of ISO 10993 (165).

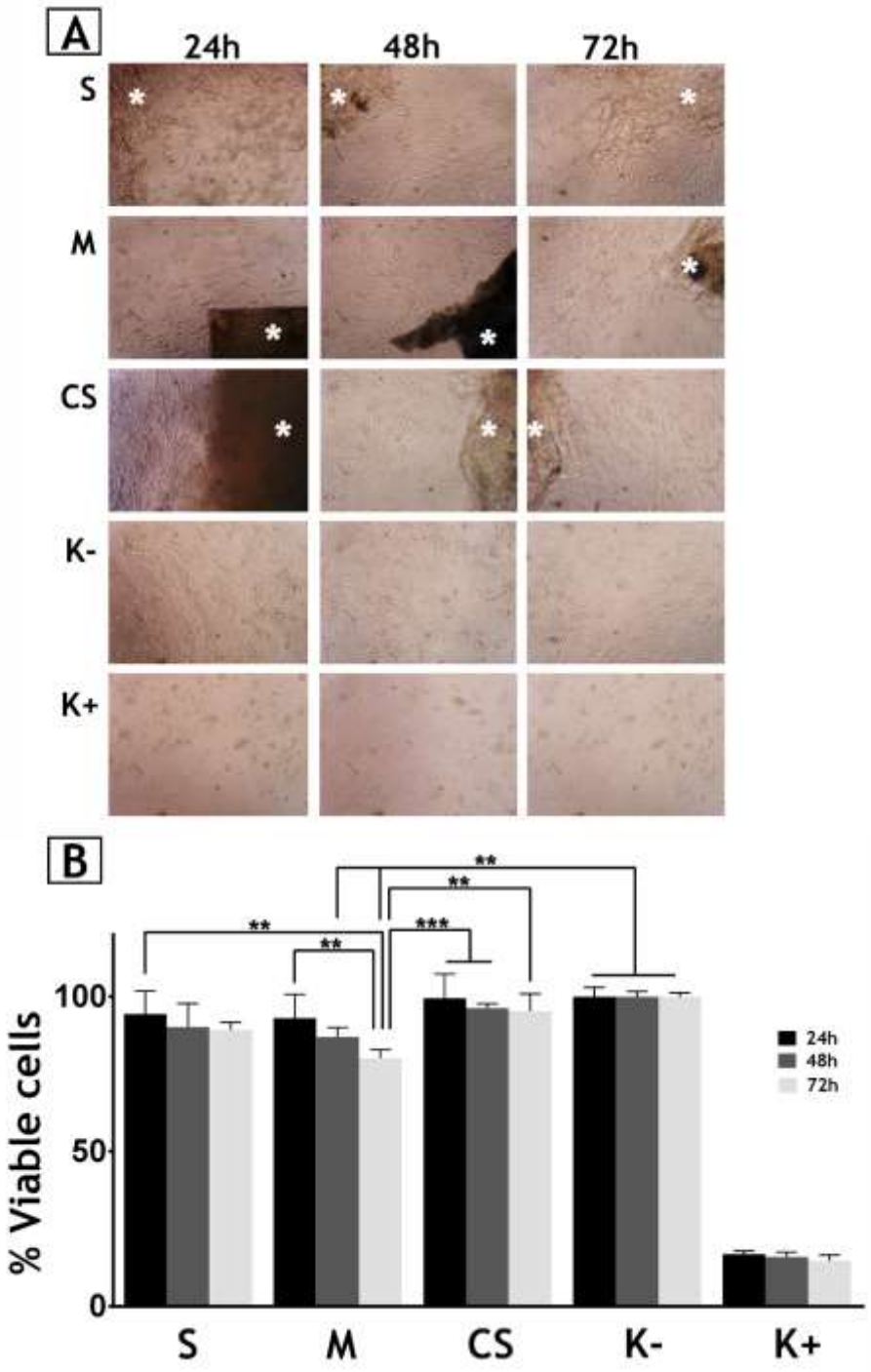

Figure 25: Characterization of cell viability in the presence of the produced materials. Microscopic images of human fibroblast cells after being seeded in the presence of the materials during 24, 48 and 72 hours (A); negative control (K-)(live cells); positive control (K+) (dead cells). Original magnification 100x. Cellular viability evaluated by on the MTT assay after 24, 48 and 72 hours is presented in (B).

3.9. Characterization of cells adhesion and penetration within produced samples

SEM analysis was also performed, to further characterize the cell adhesion and proliferation at the surface of the S, M and CS (Figure 26). Filopoidia was observed at 48 and 72 hours in the surface of the produced materials (Figure 26).

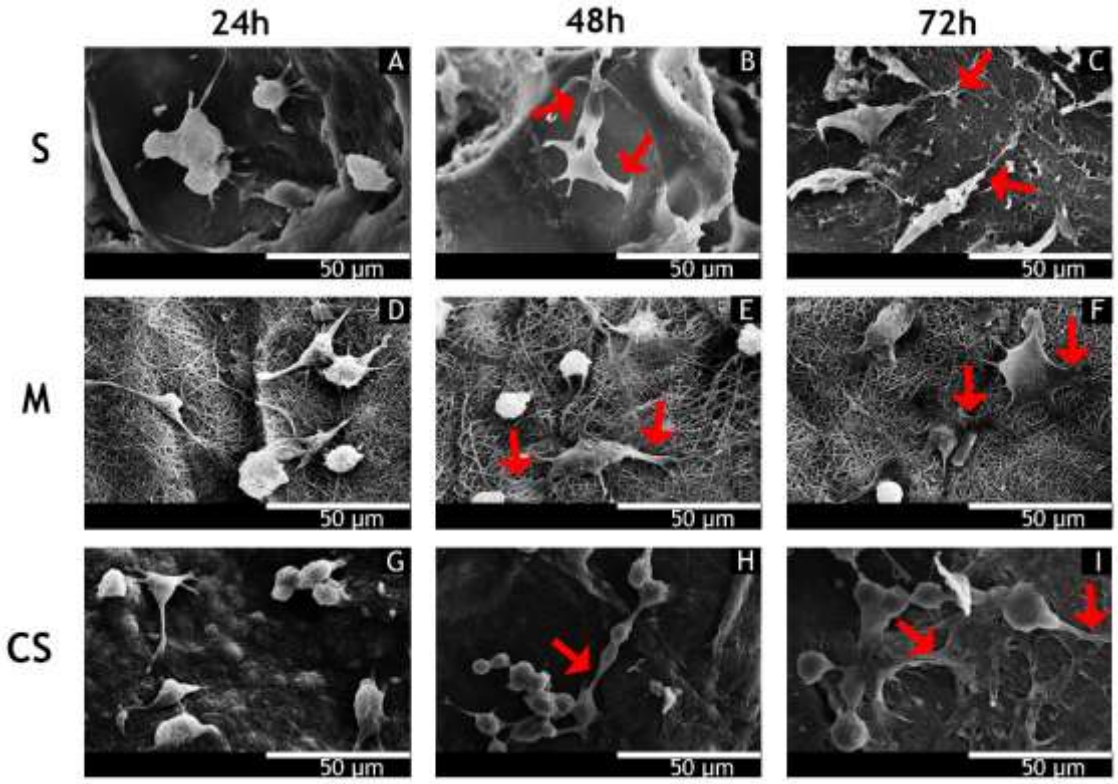

Figure 26: SEM images of NHDF in contact with S, M, and CS after 24, 48 and 72 hours. Arrows indicate cells at the surface of the materials.

The interaction between cells and sponges is mediated by integrins, which recognize specific motifs at materials surface like RGD sequences of Gelatin.

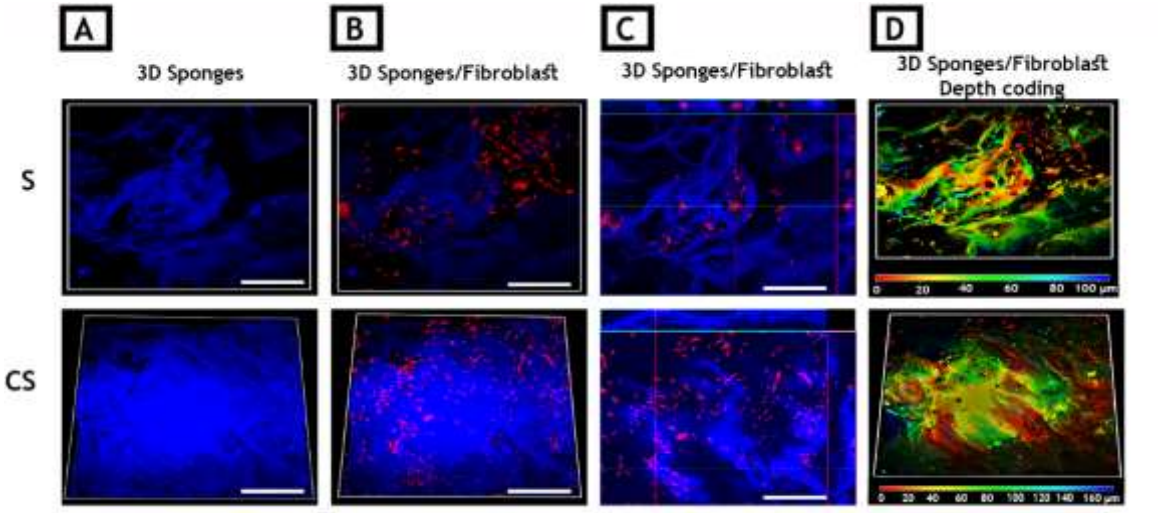

Figure 27: Characterization of cellular internalization in different sponges. The blue color represented Chitosan because it emits fluorescence and the red points are represent cells that were labeled with PI. Scale bar: 200 µm.

CLSM allows the acquisition of high-resolution optical images. The principle behind CLSM is to use a focused laser beam through a sample and then collect the reflected or emitted light from the sample, while removing any light originated from the outside of the focal point of the laser beam. The CLSM can collect images of individual slices using fluorescence or reflection from a sample in the xy, xz and yz planes (166). Through the analysis of CLSM images obtained (Figure 27) it was concluded that cells penetrate into sponges, as described in the topic 2.2.4.4.

3.10 Determination of the concentration of Ibuprofen that must be used to improve wound healing

The IC50 of a drug is the minimum concentration that is able to kill half of the population of cells (167). Therefore, the IC50 of Ibuprofen was determined in order to know the concentration of drug that could be used without killing 50 % the cells. Figure 28 A shows that the 50 % viable cells is around 0.75 to 0.80 mg/mL of the Ibuprofen. Therefore the IC50 of Ibuprofen was determined (Figure 28 B). Experimental IC50 was calculated through the fitting a the experimental data and a value of 819.58 ± 2.42 µg/mL, was determined by Origin software. Should be noted that R^2 0.99 and Chi^2 0.5 values obtained in this IC50 curve fit provide a high confidence in the obtained results.

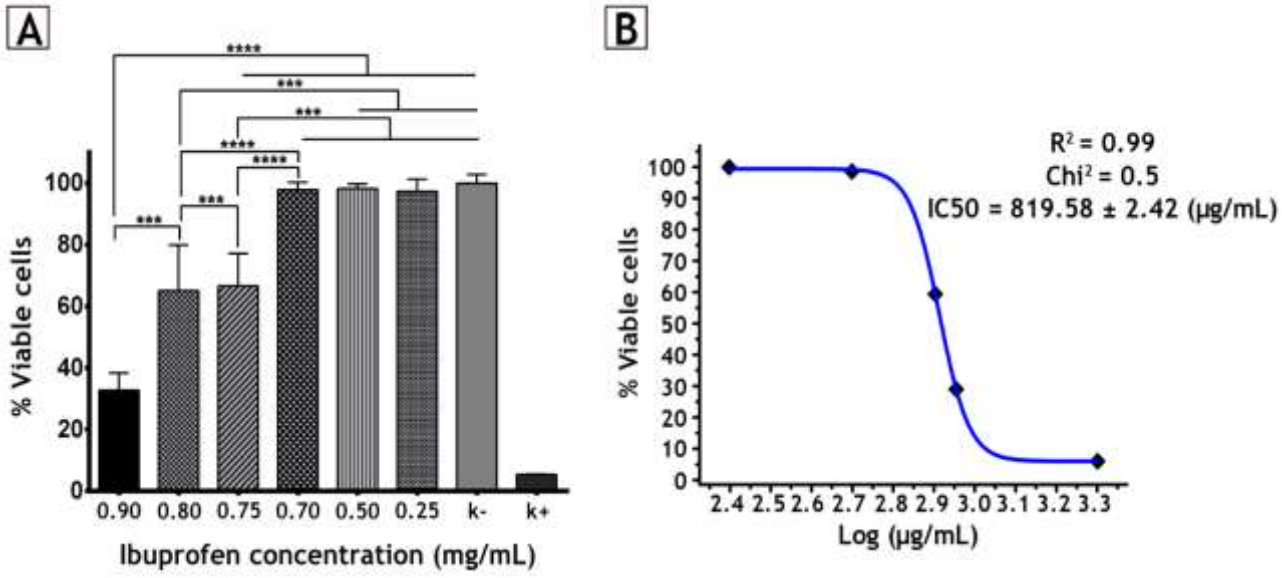

Figure 28: Evaluation of the cellular viability in contact of Ibuprofen (A). Determination of the IC50 of Ibuprofen in contact with NHDF. Blue curve represents the mathematical fitting performed for IC50 calculation. n=5.

3.11 Determination of the release profile of Ibuprofen from coated sponge

The porous sponges produced herein can be used as a drug delivery system from which drugs are released by diffusion along time (168). In order to verify if the amount of drug released is toxic for cells, the release profile of Ibuprofen was studied. The assay involved the collecting of dipping solutions that were in contact with CS and maintained at 37 ° C, pH 7.4, at 5, 10, 24, 28, 30, 46 and 50 hours. Its absorbance was determined at 264 nm in order to characterize the release profile of Ibuprofen (169). The calibration curve of Ibuprofen was performed using different concentrations (Figure 29). During the 50 hours only about 20 % of Ibuprofen loaded in sponges was released, suggesting that the drug remained trapped in the fibers (Figure 30).

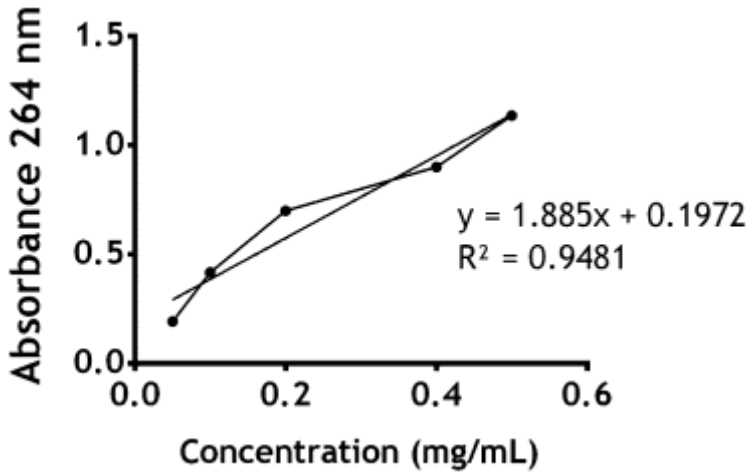

Figure 29: Representation of the calibration curves of Ibuprofen where different concentrations of the drug were used. Absorbance was determined at 264 nm.

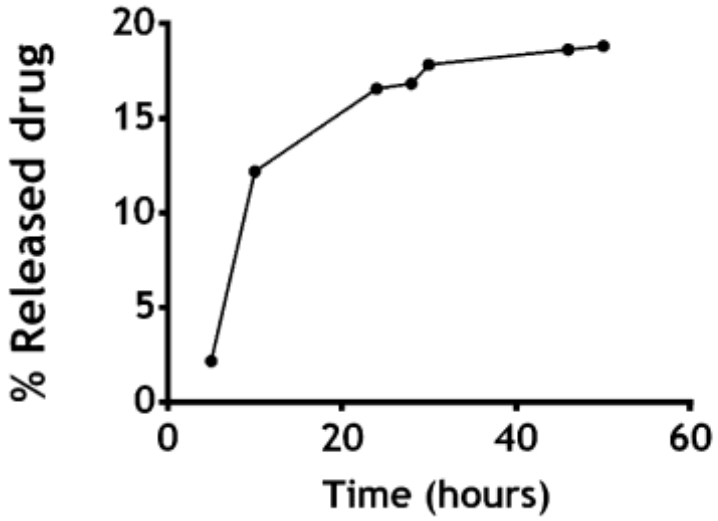

Figure 30: Characterization of the release profile of Ibuprofen. Absorbance was determined at 264 nm.

3.12 Determination of the cellular viability in contact with coated sponges loaded with Ibuprofen

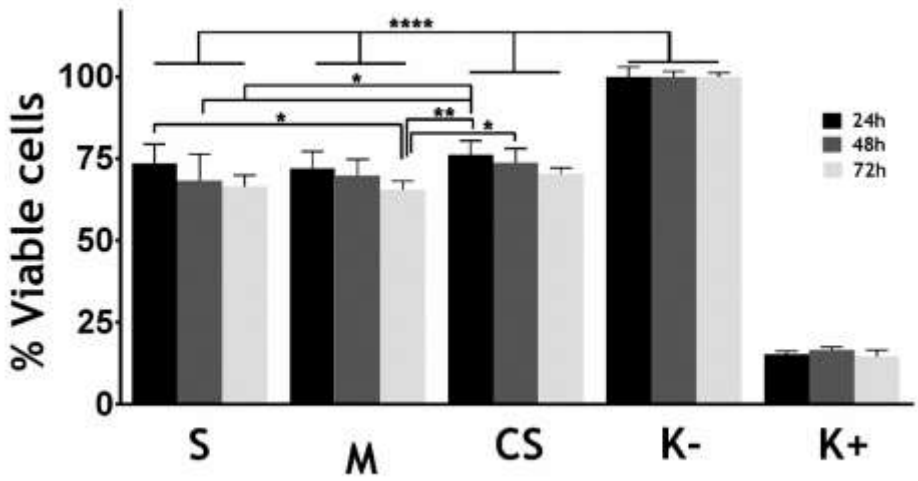

Figure 31: Determination of the cellular viability in contact with Ibuprofen loaded on S, M and CS. The negative control (K-)(live cells); positive control (K+) (dead cells).

The results obtained revealed that 65-75 % of cells remaned viable after 72 hours, when they were in contact with materials loaded with Ibuprofen (Figure 31). Taking into account the IC50 of Ibuprofen that was previously determined (Figure 28 B), a concentration of 0.8 mg/mL of Ibuprofen was incorporated in each of the sponges. However, due to the obtained results, it is necessary to use a lower Ibuprofen concentration to increase cellular viability when cells are in contact with sponges.

3.13 Evaluation of antimicrobial activity of the sponge and coated sponge

The antibacterial properties of the materials produced here were evaluated using, *Staphylococcus aureus* as model bacteria (Figure 32). This bacteria is considered appropriate to test the antibacterial properties of the sponges, since it is the most common pathogen found in skin infections.

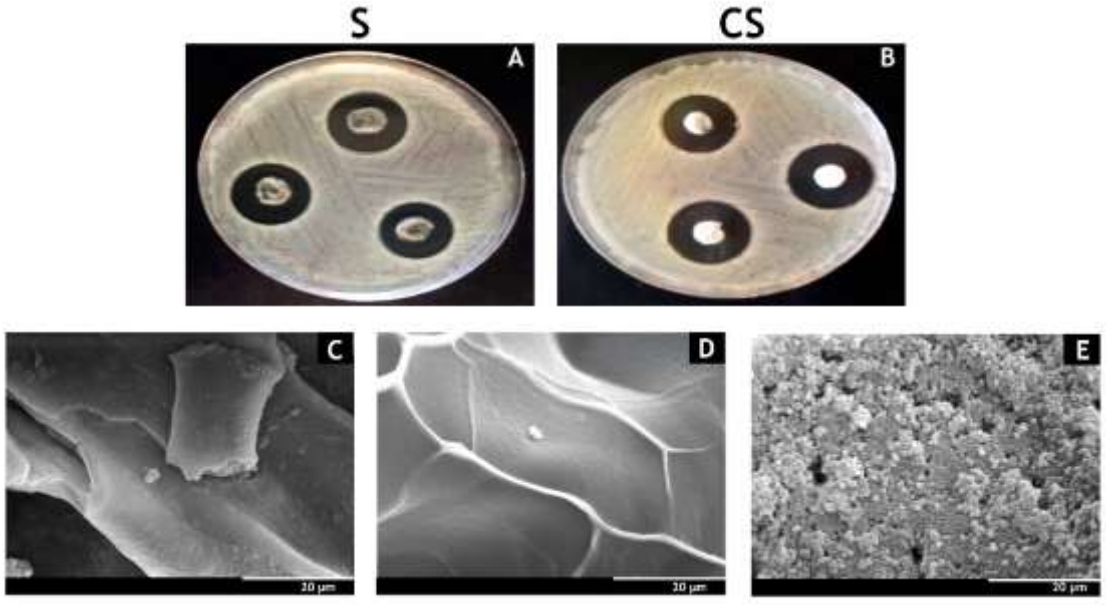

Figure 32: Evaluation of the antimicrobial properties of the produced sponges. Macroscopic images of the S and CS show the formation of an inhibitory halo (A and B); SEM images show that nobiofilm was formed on sponge surface (C and D); The negative control (*Staphylococcus aureus* grown in agar plate)) in present in (E).

In order to assess biofilm formation on the surface of the material, SEM images were also acquired (Figure 32 C and 32 D). In the case of the S it can be observed that the formation of an inhibition zone (Figure 32 A). Regarding CS can also observe the formation of an inhibitory halo was also observed (Figure 32 B), however the diameter of the halo is relatively greater then that of S. For both materials no biofilm formation was observed on their surface on the surface. The S and CS produced here showed in skin regeneration.

Chapter IV- Conclusion

4. Conclusion

Wound healing is a major worldwide health problem that particularly affects the elderly and diabetic population. In recent years, different therapeutic approaches have been proposed for improving the wound healing process. Among the different dressings developed so far, sponges that mimic the ECM have emerged as platforms that can trigger specific cellular responses at the molecular level. These wound dressings not only provide a favourable 3D microenvironment for cell adhesion and proliferation, but also allows gas, nutrients and waste products diffusion. Furthermore, these 3D matrices also confer protection to the wound from possible secondary bacterial infection.

In this study, non-toxic, highly porous and with antibactericidal activity sponges were produced using a mixture of two biocompatible natural polysaccharides (Chitosan (MMW) and Gelatin). Sponges were also coated with a nanofibrous membrane. This coating was intended to increase contact surfaces of the material in order to increase cell interaction with sponges and also reproduce layers of skin.

The obtained results revealed that S and CS promote the formation of a consistent 3D structure that supports cell adhesion and proliferation. In addition, SEM and CLSM analysis of sponges seeded with NHDF cells showed that cells were able to adhere and proliferate which is fundamental for a more rapid healing process be obtained.

Cell viability was evaluated through a MTT assay and the results confirm that the cells remain viable in contact with the sponges. Moreover, their antimicrobial activity was also assessed by the formation of inhibitory halos and of biofilm on the surface of the sponges. Thus, it can be concluded that, based on our in vitro studies, the sponges are biocompatible and that they have properties that are compatible with their application as a wound dressings.

Chapter V- Bibliography

1. Brigger I, Dubernet C, Couvreur P. Nanoparticles in cancer therapy and diagnosis. Advanced drug delivery reviews. 2002;54(5):631-51.
2. Clark RA, Ghosh K, Tonnesen MG. Tissue engineering for cutaneous wounds. Journal of Investigative Dermatology. 2007;127(5):1018-29.
3. Rodrigues AP, Saraiva Sanchez EM, da Costa AC, Moraes ÂM. The influence of preparation conditions on the characteristics of chitosan-alginate dressings for skin lesions. Journal of applied polymer science. 2008;109(4):2703-10.
4. Alemdaroğlu C, Değim Z, Çelebi N, Zor F, Öztürk S, Erdoğan D. An investigation on burn wound healing in rats with chitosan gel formulation containing epidermal growth factor. Burns. 2006;32(3):319-27.
5. Gurtner GC, Werner S, Barrandon Y, Longaker MT. Wound repair and regeneration. Nature. 2008;453(7193):314-21.
6. Kirker KR, Luo Y, Nielson JH, Shelby J, Prestwich GD. Glycosaminoglycan hydrogel films as bio-interactive dressings for wound healing. Biomaterials. 2002;23(17):3661-71.
7. Desai TA. Micro-and nanoscale structures for tissue engineering constructs. Medical Engineering & Physics. 2000;22(9):595-606.
8. Huebsch N, Mooney DJ. Inspiration and application in the evolution of biomaterials. Nature. 2009;462(7272):426-32.
9. Martin P. Wound healing--aiming for perfect skin regeneration. Science. 1997;276(5309):75-81.
10. Gauglitz GG, Schauber J. Skin: Architecture and Function. Dermal Replacements in General, Burn, and Plastic Surgery: Springer; 2013. p. 1-11.
11. Kondo T, Ishida Y. Molecular pathology of wound healing. Forensic science international. 2010;203(1):93-8.
12. Pereira RF, Barrias CC, Granja PL, Bartolo PJ. Advanced biofabrication strategies for skin regeneration and repair. Nanomedicine. 2013;8(4):603-21.
13. Brohem CA, da Silva Cardeal LB, Tiago M, Soengas MS, de Moraes Barros SB, Maria-Engler SS. Artificial skin in perspective: concepts and applications. Pigment cell & melanoma research. 2011;24(1):35-50.
14. Zhang Z, Michniak-Kohn BB. Tissue engineered human skin equivalents. Pharmaceutics. 2012;4(1):26-41.
15. Metcalfe AD, Ferguson MW. Bioengineering skin using mechanisms of regeneration and repair. Biomaterials. 2007;28(34):5100-13.
16. Böttcher-Haberzeth S, Biedermann T, Reichmann E. Tissue engineering of skin. Burns. 2010;36(4):450-60.
17. MacNeil S. Biomaterials for tissue engineering of skin. Materials today. 2008;11(5):26-35.
18. Wong DJ, Chang HY. Skin tissue engineering. StemBook 2009:3.
19. Scheuplein RJ. Permeability of the skin. Comprehensive Physiology. 2011: 299-232.
20. Balasubramani M, Kumar TR, Babu M. Skin substitutes: a review. Burns. 2001;27(5):534-44.
21. Young B, Woodford P, O'Dowd G. Wheater's functional histology: a text and colour atlas: Elsevier Health Sciences; 2013.
22. Bensouilah J, Buck P. Aromadermatology: aromatherapy in the treatment and care of common skin conditions: Radcliffe Publishing; 2006.
23. Inoue S, Reinisch C, Tschachler E, Eckhart L. Ultrastructural characterization of an artificial basement membrane produced by cultured keratinocytes. Journal of Biomedical Materials Research Part A. 2005;73(2):158-64.
24. Tate P, Seeley RR. Seeley's principles of anatomy & physiology: McGraw-Hill; 2009.
25. Zhong S, Zhang Y, Lim C. Tissue scaffolds for skin wound healing and dermal reconstruction. Wiley Interdisciplinary Reviews: Nanomedicine and Nanobiotechnology. 2010;2(5):510-25.
26. McGrath J, Eady R, Pope F. Anatomy and organization of human skin. Rook's textbook of dermatology. 2010;1.
27. Shingel KI, Faure MP, Azoulay L, Roberge C, Deckelbaum RJ. Solid emulsion gel as a vehicle for delivery of polyunsaturated fatty acids: implications for tissue repair, dermal angiogenesis and wound healing. Journal of tissue engineering and regenerative medicine. 2008;2(7):383-93.
28. Boateng JS, Matthews KH, Stevens HN, Eccleston GM. Wound healing dressings and drug delivery systems: a review. Journal of pharmaceutical sciences. 2008;97(8):2892-923.

29. Strecker-McGraw MK, Jones TR, Baer DG. Soft tissue wounds and principles of healing. Emergency medicine clinics of North America. 2007;25(1):1-22.
30. Han X, Gelein R, Corson N, Wade-Mercer P, Jiang J, Biswas P, et al. Validation of an LDH assay for assessing nanoparticle toxicity. Toxicology. 2011;287(1):99-104.
31. Valente J, Valente T, Alves P, Ferreira P, Silva A, Correia I. Alginate based scaffolds for bone tissue engineering. Materials Science and Engineering: C. 2012;32(8):2596-603.
32. Ko J, Park H, Hwang S, Park J, Lee J. Preparation and characterization of chitosan microparticles intended for controlled drug delivery. International journal of pharmaceutics. 2002;249(1):165-74.
33. Supp DM, Boyce ST. Engineered skin substitutes: practices and potentials. Clinics in dermatology. 2005;23(4):403-12.
34. Shevchenko RV, James SL, James SE. A review of tissue-engineered skin bioconstructs available for skin reconstruction. Journal of the Royal Society Interface. 2010;7(43):229-58.
35. Enoch S, Leaper DJ. Basic science of wound healing. Surgery (Oxford). 2008;26(2):31-7.
36. Burd A, Ayyappan T, Huang L. Cord blood: opportunities and challenges for the reconstructive surgeon. Frontiers of Cord Blood Science: Springer; 2009. p. 273-87.
37. Steffens D, Leonardi D, Soster PRdL, Lersch M, Rosa A, Crestani T, et al. Development of a new nanofiber scaffold for use with stem cells in a third degree burn animal model. Burns. 2014; 40:1650–1660.
38. Paul W, Sharma CP. Chitosan and alginate wound dressings: a short review. Trends Biomater Artif Organs. 2004;18(1):18-23.
39. Auger FA, Berthod F, Moulin V, Pouliot R, Germain L. Tissue-engineered skin substitutes: from in vitro constructs to in vivo applications. Biotechnology and applied biochemistry. 2004;39(3):263-75.
40. Torpy JM, Lynm C, Glass RM. Burn Injuries. JAMA. 2009;302(16):1828-.
41. Tonnesen MG, Feng X, Clark RA, editors. Angiogenesis in wound healing. Journal of Investigative Dermatology Symposium Proceedings; Nature Publishing Group 2000; 5(1): 40–46.
42. Reinke J, Sorg H. Wound repair and regeneration. European Surgical Research. 2012;49(1):35-43.
43. Behm B, Babilas P, Landthaler M, Schreml S. Cytokines, chemokines and growth factors in wound healing. Journal of the European Academy of Dermatology and Venereology. 2012;26(7):812-20.
44. Beldon P. Basic science of wound healing. Surgery (Oxford). 2010;28(9):409-12.
45. Velnar T, Bailey T, Smrkolj V. The wound healing process: an overview of the cellular and molecular mechanisms. Journal of International Medical Research. 2009;37(5):1528-42.
46. Zieske JD. Extracellular matrix and wound healing. Current opinion in ophthalmology. 2001;12(4):237-41.
47. Lee KY, Peters MC, Anderson KW, Mooney DJ. Controlled growth factor release from synthetic extracellular matrices. Nature. 2000;408(6815):998-1000.
48. Guo S, DiPietro LA. Factors affecting wound healing. Journal of dental research. 2010;89(3):219-29.
49. Strodtbeck F. Physiology of wound healing. Newborn and infant nursing reviews. 2001;1(1):43-52.
50. Li J, Chen J, Kirsner R. Pathophysiology of acute wound healing. Clinics in dermatology. 2007;25(1):9-18.
51. Nauta A, Gurtner G, Longaker M. Wound healing and regenerative strategies. Oral diseases. 2011;17(6):541-9.
52. Harrison BS, Atala A. Carbon nanotube applications for tissue engineering. Biomaterials. 2007;28(2):344-53.
53. Norman JJ, Desai TA. Methods for fabrication of nanoscale topography for tissue engineering scaffolds. Annals of biomedical engineering. 2006;34(1):89-101.
54. Ma L, Gao C, Mao Z, Zhou J, Shen J, Hu X, et al. Collagen/chitosan porous scaffolds with improved biostability for skin tissue engineering. Biomaterials. 2003;24(26):4833-41.
55. Ohashi K, Yokoyama T, Yamato M, Kuge H, Kanehiro H, Tsutsumi M, et al. Engineering functional two-and three-dimensional liver systems in vivo using hepatic tissue sheets. Nature medicine. 2007;13(7):880-5.
56. Tziampazis E, Sambanis A. Tissue engineering of a bioartificial pancreas: modeling the cell environment and device function. Biotechnology progress. 1995;11(2):115-26.

57. Chen MK, Badylak SF. Small bowel tissue engineering using small intestinal submucosa as a scaffold. Journal of Surgical Research. 2001;99(2):352-8.
58. Zhu Y, Chian KS, Chan-Park MB, Mhaisalkar PS, Ratner BD. Protein bonding on biodegradable poly (L-lactide-co-caprolactone) membrane for esophageal tissue engineering. Biomaterials. 2006;27(1):68-78.
59. Ghasemi-Mobarakeh L, Prabhakaran MP, Morshed M, Nasr-Esfahani M-H, Ramakrishna S. Electrospun poly (ε-caprolactone)/gelatin nanofibrous scaffolds for nerve tissue engineering. Biomaterials. 2008;29(34):4532-9.
60. Freed L, Vunjak-Novakovic G. Tissue engineering of cartilage. The biomedical engineering handbook. 2000;1.
61. Hutmacher DW. Scaffolds in tissue engineering bone and cartilage. Biomaterials. 2000;21(24):2529-43.
62. Caoa Y, Vacanti J, Ma P, Ibarra C, Paige K, Upton J, et al., editors. Tissue engineering of tendon. MRS Proceedings; 1995: Cambridge Univ Press.
63. Kelton Jr PL. Skin grafts and skin substitutes. Selected Readings in Plastic Surgery. 1999;9(1):1-24.
64. Queen D, Evans J, Gaylor J, Courtney J, Reid W. Burn wound dressings—a review. Burns. 1987;13(3):218-28.
65. Babensee JE, Anderson JM, McIntire LV, Mikos AG. Host response to tissue engineered devices. Advanced drug delivery reviews. 1998;33(1):111-39.
66. Ribeiro MP, Espiga A, Silva D, Baptista P, Henriques J, Ferreira C, et al. Development of a new chitosan hydrogel for wound dressing. Wound Repair and Regeneration. 2009;17(6):817-24.
67. Kumbar SG, Nukavarapu SP, James R, Nair LS, Laurencin CT. Electrospun poly (lactic acid-< i> co</i>-glycolic acid) scaffolds for skin tissue engineering. Biomaterials. 2008;29(30):4100-7.
68. Gomes S, Leonor IB, Mano JF, Reis RL, Kaplan DL. Natural and genetically engineered proteins for tissue engineering. Progress in polymer science. 2012;37(1):1-17.
69. Auger F, Lacroix D, Germain L. Skin substitutes and wound healing. Skin pharmacology and physiology. 2008;22(2):94-102.
70. Yang S, Leong K-F, Du Z, Chua C-K. The design of scaffolds for use in tissue engineering. Part I. Traditional factors. Tissue engineering. 2001;7(6):679-89.
71. Kim I-Y, Seo S-J, Moon H-S, Yoo M-K, Park I-Y, Kim B-C, et al. Chitosan and its derivatives for tissue engineering applications. Biotechnology advances. 2008;26(1):1-21.
72. Franco RA, Nguyen TH, Lee B-T. Preparation and characterization of electrospun PCL/PLGA membranes and chitosan/gelatin hydrogels for skin bioengineering applications. Journal of Materials Science: Materials in Medicine. 2011;22(10):2207-18.
73. Bello YM, Falabella AF, Eaglstein WH. Tissue-engineered skin. American journal of clinical dermatology. 2001;2(5):305-13.
74. Jones I, Currie L, Martin R. A guide to biological skin substitutes. British journal of plastic surgery. 2002;55(3):185-93.
75. Horch RE. Tissue Engineering of Cultured Skin Substitutes. Fundamentals of Tissue Engineering and Regenerative Medicine: Springer; 2009. p. 329-43.
76. Atiyeh BS, Gunn SW, Hayek SN. State of the art in burn treatment. World journal of surgery. 2005;29(2):131-48.
77. Cichowski A, Kawecki M, Glik J, Klama-Baryła A, Łabuś W, Maj M, et al. Literature Review Concerning Cell and Skin Substitute Cultures Obtained by Means of Tissue Engineering used in the Treatment of Burns. Polish Journal of Surgery. 2014;86(4):202-10.
78. Anthony ET, Syed M, Myers S, Moir G, Navsaria H. The development of novel dermal matrices for cutaneous wound repair. Drug Discovery Today: Therapeutic Strategies. 2006;3(1):81-6.
79. Marston WA, Hanft J, Norwood P, Pollak R. The Efficacy and Safety of Dermagraft in Improving the Healing of Chronic Diabetic Foot Ulcers Results of a prospective randomized trial. Diabetes Care. 2003;26(6):1701-5.
80. Shakespeare PG. The role of skin substitutes in the treatment of burn injuries. Clinics in dermatology. 2005;23(4):413-8.
81. Pham C, Greenwood J, Cleland H, Woodruff P, Maddern G. Bioengineered skin substitutes for the management of burns: a systematic review. Burns. 2007;33(8):946-57.

82. Monteiro IP, Shukla A, Marques AP, Reis RL, Hammond PT. Spray-assisted layer-by-layer assembly on hyaluronic acid scaffolds for skin tissue engineering. Journal of Biomedical Materials Research Part A. 2014.
83. Bhat S, Kumar A. Cell proliferation on three-dimensional chitosan–agarose–gelatin cryogel scaffolds for tissue engineering applications. Journal of bioscience and bioengineering. 2012;114(6):663-70.
84. Chen G, Ushida T, Tateishi T. Scaffold design for tissue engineering. Macromolecular Bioscience. 2002;2(2):67-77.
85. O'Brien FJ. Biomaterials & scaffolds for tissue engineering. Materials Today. 2011;14(3):88-95.
86. Collins MN, Birkinshaw C. Hyaluronic acid based scaffolds for tissue engineering—A review. Carbohydrate polymers. 2013;92(2):1262-79.
87. Oliveira MB, Mano JF. Polymer-based microparticles in tissue engineering and regenerative medicine. Biotechnology progress. 2011;27(4):897-912.
88. Lebourg M, Serra RS, Estellés JM, Sánchez FH, Ribelles JG, Antón JS. Biodegradable polycaprolactone scaffold with controlled porosity obtained by modified particle-leaching technique. Journal of Materials Science: Materials in Medicine. 2008;19(5):2047-53.
89. Liapis A, Pim M, Bruttini R. Research and development needs and opportunities in freeze drying. Drying technology. 1996;14(6):1265-300.
90. Kulkarni A, Bambole V, Mahanwar P. Electrospinning of polymers, their modeling and applications. Polymer-Plastics Technology and Engineering. 2010;49(5):427-41.
91. Bhardwaj N, Kundu SC. Electrospinning: a fascinating fiber fabrication technique. Biotechnology advances. 2010;28(3):325-47.
92. Moghe A, Gupta B. Co-axial Electrospinning for Nanofiber Structures: Preparation and Applications. Polymer Reviews. 2008;48(2):353-77.
93. Elias KL, Price RL, Webster TJ. Enhanced functions of osteoblasts on nanometer diameter carbon fibers. Biomaterials. 2002;23(15):3279-87.
94. Supaphol P, Suwantong O, Sangsanoh P, Srinivasan S, Jayakumar R, Nair SV. Electrospinning of biocompatible polymers and their potentials in biomedical applications. Biomedical applications of polymeric nanofibers: Springer; 2012. p. 213-39.
95. Sill TJ, von Recum HA. Electrospinning: applications in drug delivery and tissue engineering. Biomaterials. 2008;29(13):1989-2006.
96. Yoo HS, Kim TG, Park TG. Surface-functionalized electrospun nanofibers for tissue engineering and drug delivery. Advanced drug delivery reviews. 2009;61(12):1033-42.
97. Li D, Wang Y, Xia Y. Electrospinning nanofibers as uniaxially aligned arrays and layer-by-layer stacked films. Advanced Materials. 2004;16(4):361-6.
98. Yusof NLBM, Wee A, Lim LY, Khor E. Flexible chitin films as potential wound-dressing materials: Wound model studies. Journal of Biomedical Materials Research Part A. 2003;66(2):224-32.
99. Khan TA, Peh KK, Ch'ng HS. Mechanical, bioadhesive strength and biological evaluations of chitosan films for wound dressing. J Pharm Pharmaceut Sci. 2000;3(3):303-11.
100. Wang L, Khor E, Wee A, Lim LY. Chitosan-alginate PEC membrane as a wound dressing: Assessment of incisional wound healing. Journal of biomedical materials research. 2002;63(5):610-8.
101. Wu Y-B, Yu S-H, Mi F-L, Wu C-W, Shyu S-S, Peng C-K, et al. Preparation and characterization on mechanical and antibacterial properties of chitsoan/cellulose blends. Carbohydrate Polymers. 2004;57(4):435-40.
102. Czaja W, Krystynowicz A, Bielecki S, Brown RM. Microbial cellulose—the natural power to heal wounds. Biomaterials. 2006;27(2):145-51.
103. Ruiz-Cardona L, Sanzgiri YD, Benedetti L, Stella VJ, Topp EM. Application of benzyl hyaluronate membranes as potential wound dressings: evaluation of water vapour and gas permeabilities. Biomaterials. 1996;17(16):1639-43.
104. Chang C-H, Liu H-C, Lin C-C, Chou C-H, Lin F-H. Gelatin–chondroitin–hyaluronan tri-copolymer scaffold for cartilage tissue engineering. Biomaterials. 2003;24(26):4853-8.
105. TANAKA A, NAGATE T, MATSUDA H. Acceleration of wound healing by gelatin film dressings with epidermal growth factor. Journal of veterinary medical science. 2005;67(9):909-13.
106. Wu Z, Sheng Z, Sun T, Geng M, Li J, Yao Y, et al. Preparation of collagen-based materials for wound dressing. Chinese medical journal. 2003;116(3):419-23.

107. Mi F-L, Wu Y-B, Shyu S-S, Chao A-C, Lai J-Y, Su C-C. Asymmetric chitosan membranes prepared by dry/wet phase separation: a new type of wound dressing for controlled antibacterial release. Journal of Membrane Science. 2003;212(1):237-54.
108. Lee Y-H, Chang J-J, Yang M-C, Chien C-T, Lai W-F. Acceleration of wound healing in diabetic rats by layered hydrogel dressing. Carbohydrate Polymers. 2012;88(3):809-19.
109. Xiao-dong G, Qi-xin Z, Jing-yuan D, Shu-hua Y, Hong W, Zeng-wu S, et al. Molecular tissue engineering: Concepts, status and challenge. Journal of Wuhan University of Technology-Mater Sci Ed. 2002;17(3):30-4.
110. Lee CH, Singla A, Lee Y. Biomedical applications of collagen. International journal of pharmaceutics. 2001;221(1):1-22.
111. Swetha M, Sahithi K, Moorthi A, Srinivasan N, Ramasamy K, Selvamurugan N. Biocomposites containing natural polymers and hydroxyapatite for bone tissue engineering. International journal of biological macromolecules. 2010;47(1):1-4.
112. Wan Y, Lu X, Dalai S, Zhang J. Thermophysical properties of polycaprolactone/chitosan blend membranes. Thermochimica Acta. 2009;487(1):33-8.
113. Bhattarai N, Edmondson D, Veiseh O, Matsen FA, Zhang M. Electrospun chitosan-based nanofibers and their cellular compatibility. Biomaterials. 2005;26(31):6176-84.
114. Sudarshan N, Hoover D, Knorr D. Antibacterial action of chitosan. Food Biotechnology. 1992;6(3):257-72.
115. Wang G-H. Inhibition and inactivation of five species of foodborne pathogens by chitosan. Journal of food protection (USA). 1992.
116. Suh J-KF, Matthew HW. Application of chitosan-based polysaccharide biomaterials in cartilage tissue engineering: a review. Biomaterials. 2000;21(24):2589-98.
117. Hutmacher D, Goh J, Teoh S. An introduction to biodegradable materials for tissue engineering applications. Annals of the Academy of Medicine, Singapore. 2001;30(2):183-91.
118. Taravel M, Domard A. Collagen and its interaction with chitosan: II. Influence of the physicochemical characteristics of collagen. Biomaterials. 1995;16(11):865-71.
119. Taravel M, Domard A. Collagen and its interactions with chitosan: III. Some biological and mechanical properties. Biomaterials. 1996;17(4):451-5.
120. Shi C, Zhu Y, Ran X, Wang M, Su Y, Cheng T. Therapeutic potential of chitosan and its derivatives in regenerative medicine. Journal of Surgical research. 2006;133(2):185-92.
121. Thein-Han W, Kitiyanant Y, Misra R. Chitosan as scaffold matrix for tissue engineering. Materials Science and Technology. 2008;24(9):1062-75.
122. Malafaya PB, Silva GA, Reis RL. Natural–origin polymers as carriers and scaffolds for biomolecules and cell delivery in tissue engineering applications. Advanced drug delivery reviews. 2007;59(4):207-33.
123. Lien S-M, Ko L-Y, Huang T-J. Effect of pore size on ECM secretion and cell growth in gelatin scaffold for articular cartilage tissue engineering. Acta Biomaterialia. 2009;5(2):670-9.
124. Rose JB, Pacelli S, Haj AJE, Dua HS, Hopkinson A, White LJ, et al. Gelatin-based materials in ocular tissue engineering. Materials. 2014;7(4):3106-35.
125. Abuknesha RA, Jeganathan F, DeGroot R, Wildeboer D, Price RG. Detection of proteases using an immunochemical method with haptenylated–gelatin as a solid-phase substrate. Analytical and bioanalytical chemistry. 2010;396(7):2547-58.
126. Son WK, Youk JH, Lee TS, Park WH. The effects of solution properties and polyelectrolyte on electrospinning of ultrafine poly (ethylene oxide) fibers. Polymer. 2004;45(9):2959-66.
127. Ferreira S. Peripheral analgesic sites of action of anti-inflammatory drugs. International journal of clinical practice Supplement. 2002(128):2-10.
128. Mitchell JA, Warner TD. Cyclo-oxygenase-2: pharmacology, physiology, biochemistry and relevance to NSAID therapy. British journal of pharmacology. 1999;128(6):1121-32.
129. Kayaalp A. Medical Pharmacology. Feryal Press Ltd., Ankara; 1992.
130. Ferraz J, Sharkey KA, Reuter BK, Asfaha S, Tigley AW, Brown ML, et al. Induction of cyclooxygenase 1 and 2 in the rat stomach during endotoxemia: role in resistance to damage. Gastroenterology. 1997;113(1):195-204.
131. Michaluart P, Masferrer JL, Carothers AM, Subbaramaiah K, Zweifel BS, Koboldt C, et al. Inhibitory effects of caffeic acid phenethyl ester on the activity and expression of cyclooxygenase-2 in human oral epithelial cells and in a rat model of inflammation. Cancer research. 1999;59(10):2347-52.

132. Siegle I, Klein T, Backman JT, Saal JG, Nüsing RM, Fritz P. Expression of cyclooxygenase 1 and cyclooxygenase 2 in human synovial tissue: differential elevation of cyclooxygenase 2 in inflammatory joint diseases. Arthritis & Rheumatism. 1998;41(1):122-9.
133. Vane JR, Mitchell JA, Appleton I, Tomlinson A, Bishop-Bailey D, Croxtall J, et al. Inducible isoforms of cyclooxygenase and nitric-oxide synthase in inflammation. Proceedings of the National Academy of Sciences. 1994;91(6):2046-50.
134. Lewis JR. Evaluation of ibuprofen (MOTRIN): A new antirheumatic agent. JAMA. 1975;233(4):364-5.
135. Brooks C, Schlagel C, Sekhar N, Sobota J. Tolerance and pharmacology of ibuprofen. Current therapeutic research, clinical and experimental. 1973;15(4):180.
136. Demling R, LaLonde C. Topical ibuprofen decreases early postburn edema. Surgery. 1987;102(5):857-61.
137. Serra I, Fradique R, Vallejo M, Correia T, Miguel S, Correia I. Production and characterization of Chitosan/Gelatin/β-TCP scaffolds for improved bone tissue regeneration. Materials Science and Engineering: C. 2015.
138. Gaspar V, Sousa F, Queiroz J, Correia I. Formulation of chitosan–TPP–pDNA nanocapsules for gene therapy applications. Nanotechnology. 2011;22(1):015101.
139. Muzzarelli RA, Rocchetti R. Determination of the degree of acetylation of chitosans by first derivative ultraviolet spectrophotometry. Carbohydrate Polymers. 1985;5(6):461-72.
140. Ionescu LC, Lee GC, Sennett BJ, Burdick JA, Mauck RL. An anisotropic nanofiber/microsphere composite with controlled release of biomolecules for fibrous tissue engineering. Biomaterials. 2010;31(14):4113-20.
141. Ma G, Fang D, Liu Y, Zhu X, Nie J. Electrospun sodium alginate/poly (ethylene oxide) core–shell nanofibers scaffolds potential for tissue engineering applications. Carbohydrate Polymers. 2012;87(1):737-43.
142. Bacsik Z, Mink J, Keresztury G. FTIR spectroscopy of the atmosphere. I. Principles and methods. Applied spectroscopy reviews. 2004;39(3):295-363.
143. Miguel SP, Ribeiro MP, Brancal H, Coutinho P, Correia IJ. Thermoresponsive chitosan–agarose hydrogel for skin regeneration. Carbohydrate polymers. 2014;111:366-73.
144. Zonari A, Cerqueira MT, Novikoff S, Goes AM, Marques AP, Correlo VM, et al. Poly (hydroxybutyrate-co-hydroxyvalerate) Bilayer Skin Tissue Engineering Constructs with Improved Epidermal Rearrangement. Macromolecular bioscience. 2014;14(7):977-90.
145. Huang Y, Onyeri S, Siewe M, Moshfeghian A, Madihally SV. In vitro characterization of chitosan–gelatin scaffolds for tissue engineering. Biomaterials. 2005;26(36):7616-27.
146. Ribeiro M, Morgado P, Miguel S, Coutinho P, Correia I. Dextran-based hydrogel containing chitosan microparticles loaded with growth factors to be used in wound healing. Materials Science and Engineering: C. 2013;33(5):2958-66.
147. Morgan DM. Tetrazolium (MTT) assay for cellular viability and activity. Polyamine protocols: Springer; 1998. p. 179-84.
148. Rasband W. ImageJ. US National Institutes of Health, Bethesda, MD, USA. 1997.
149. Qin C, Du Y, Xiao L, Li Z, Gao X. Enzymic preparation of water-soluble chitosan and their antitumor activity. International journal of biological macromolecules. 2002;31(1):111-7.
150. Değim Z, Celebi N, Sayan H, Babül A, Erdoğan D, Take G. An investigation on skin wound healing in mice with a taurine-chitosan gel formulation. Amino acids. 2002;22(2):187-98.
151. Rabea EI, Badawy ME-T, Stevens CV, Smagghe G, Steurbaut W. Chitosan as antimicrobial agent: applications and mode of action. Biomacromolecules. 2003;4(6):1457-65.
152. Kim KW, Thomas R, Lee C, Park HJ. Antimicrobial activity of native chitosan, degraded chitosan, and O-carboxymethylated chitosan. Journal of Food Protection®. 2003;66(8):1495-8.
153. Yuan Y, Chesnutt BM, Haggard WO, Bumgardner JD. Deacetylation of chitosan: Material characterization and in vitro evaluation via albumin adsorption and pre-osteoblastic cell cultures. Materials. 2011;4(8):1399-416.
154. Antunes B, Moreira A, Gaspar V, Correia I. Chitosan/arginine–chitosan polymer blends for assembly of nanofibrous membranes for wound regeneration. Carbohydrate Polymers. 2015;130:104-12.
155. Chong E, Phan T, Lim I, Zhang Y, Bay B, Ramakrishna S, et al. Evaluation of electrospun PCL/gelatin nanofibrous scaffold for wound healing and layered dermal reconstitution. Acta biomaterialia. 2007;3(3):321-30.
156. Hodgkinson T, Yuan X-F, Bayat A. Electrospun silk fibroin fiber diameter influences in vitro dermal fibroblast behavior and promotes healing of ex vivo wound models. Journal of tissue engineering. 2014;5:2041731414551661.

157. Lim S-H, Hudson SM. Synthesis and antimicrobial activity of a water-soluble chitosan derivative with a fiber-reactive group. Carbohydrate research. 2004;339(2):313-9.
158. Bhat S, Tripathi A, Kumar A. Supermacroprous chitosan–agarose–gelatin cryogels: in vitro characterization and in vivo assessment for cartilage tissue engineering. Journal of the Royal Society Interface. 2011;8(57):540-54.
159. Manzano M, Aina V, Arean C, Balas F, Cauda V, Colilla M, et al. Studies on MCM-41 mesoporous silica for drug delivery: effect of particle morphology and amine functionalization. Chemical Engineering Journal. 2008;137(1):30-7.
160. Mihaila SM, Gaharwar AK, Reis RL, Marques AP, Gomes ME, Khademhosseini A. Photocrosslinkable Kappa-Carrageenan Hydrogels for Tissue Engineering Applications. Advanced healthcare materials. 2013;2(6):895-907.
161. Nichol JW, Koshy ST, Bae H, Hwang CM, Yamanlar S, Khademhosseini A. Cell-laden microengineered gelatin methacrylate hydrogels. Biomaterials. 2010;31(21):5536-44.
162. Yang C, Xu L, Zhou Y, Zhang X, Huang X, Wang M, et al. A green fabrication approach of gelatin/CM-chitosan hybrid hydrogel for wound healing. Carbohydrate Polymers. 2010;82(4):1297-305.
163. Pasparakis G, Bouropoulos N. Swelling studies and in vitro release of verapamil from calcium alginate and calcium alginate–chitosan beads. International journal of pharmaceutics. 2006;323(1):34-42.
164. Ananthanarayanan B, Kim Y, Kumar S. Elucidating the mechanobiology of malignant brain tumors using a brain matrix-mimetic hyaluronic acid hydrogel platform. Biomaterials. 2011;32(31):7913-23.
165. Desai LS, Lister L. Biocompatibility Safety Assessment of Medical Devices: FDA/ISO and Japanese Guidelines.
166. Paddock SW. Confocal laser scanning microscopy. Biotechniques. 1999;27:992-1007.
167. Zhou Wj, Zhang X, Cheng C, Wang F, Wang Xk, Liang Yj, et al. Crizotinib (PF-02341066) reverses multidrug resistance in cancer cells by inhibiting the function of P-glycoprotein. British journal of pharmacology. 2012;166(5):1669-83.
168. Berger J, Reist M, Mayer JM, Felt O, Peppas N, Gurny R. Structure and interactions in covalently and ionically crosslinked chitosan hydrogels for biomedical applications. European Journal of Pharmaceutics and Biopharmaceutics. 2004;57(1):19-34.
169. Kolhe P, Misra E, Kannan RM, Kannan S, Lieh-Lai M. Drug complexation, in vitro release and cellular entry of dendrimers and hyperbranched polymers. International Journal of Pharmaceutics. 2003;259(1):143-60.